Study on The Thermal Transition of Collagen Model Peptides in Solution

Susumu Uchiyama

Faculty of Pharmaceuical Sciences
Osaka University

1999

Study on the thermal transition of collagen model peptides in solution

A Doctoral Thesis
Submitted to the Graduate School of Pharmaceutical Sciences
Osaka University

Susumu Uchiyama

1999

Contents

Chapter IV

The partial molar volume of collagen model peptides

General Introduction

The collagens are a family of the fibrous proteins that are widely distributed throughout multicellular animals [1]. They are the major proteins of the extracellular matrix, such as skin and bone, and form higher order structures unique to the location in which they are expressed. Recently, collagens have been applied to industrial uses as useful biomaterials and thus have received much attention.

One of the characteristic features of a typical collagen molecule is that it forms, long and hard, rod like triple helix structure [1-3]. The triple helix is one of the typical structural motifs of proteins and is found not only in collagens but also in other proteins, such as C1q or macrophage scavenger receptor [4,5]. In the triple helix, three polypeptide chains, each of which has left handed polyproline II like conformation, fold together in a right-handed manner (Fig. 1).

The amino acid sequence found in proteins or peptides which form triple helix is the repeating of a (X-Y-Gly) triplet, where imino acids such as proline or hydroxyproline are often seen in the X or Y positions [6]. This repeating of the (X-Y-Gly) triplet is essential to stabilize the triple helix structure. Glycine is the only amino acid that can be accommodated in the compact structure of the triple helix. The ring structure of the proline or hydroxyproline residue in triple helix confers the stiffness to each constituting chain and it assists triple helix formation.

In 1970, Kobayashi et al. found that the chemically synthesized polytripeptides, $(Pro\text{-}Pro\text{-}Gly)_n$ and $(Pro\text{-}Hyp\text{-}Gly)_n$ (n=10,15), form trimers in solution and found that their molecular weight decreased to that of monomer with

Fig. 1. The triple-stranded collagen helix.

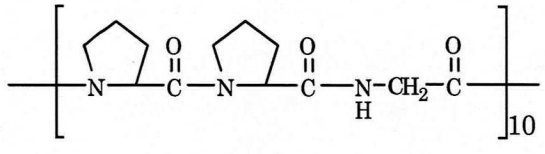

$(Pro\text{-}Pro\text{-}Gly)_{10}$

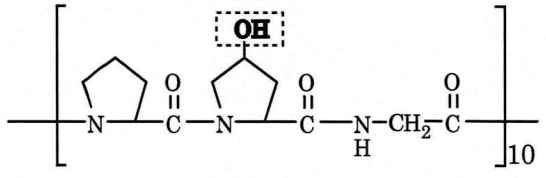

$(Pro\text{-}Hyp\text{-}Gly)_{10}$

Fig. 2. Structures of $(Pro\text{-}Pro\text{-}Gly)_{10}$ and $(Pro\text{-}Hyp\text{-}Gly)_{10}$.

increasing temperature (Fig. 2 and 3) [7]. They also found the transition temperature of $(Pro\text{-}Hyp\text{-}Gly)_{10}$ is about 60 °C, which is 30 °C higher than that of $(Pro\text{-}Pro\text{-}Gly)_{10}$ (Fig. 4) [8]. After these findings, $(Pro\text{-}Pro\text{-}Gly)_n$ and $(Pro\text{-}Hyp\text{-}Gly)_n$ were commonly acknowledged to be typical collagen model peptides [9]. Generally, physico-chemical studies using collagens are difficult because even a collagen mol-

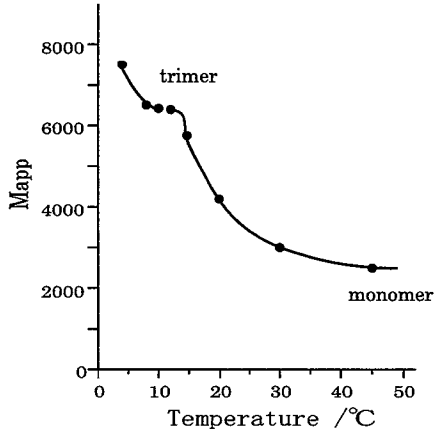

Fig. 3. Temperature dependence of M_{app} of $(Pro\text{-}Pro\text{-}Gly)_{10}$[7].

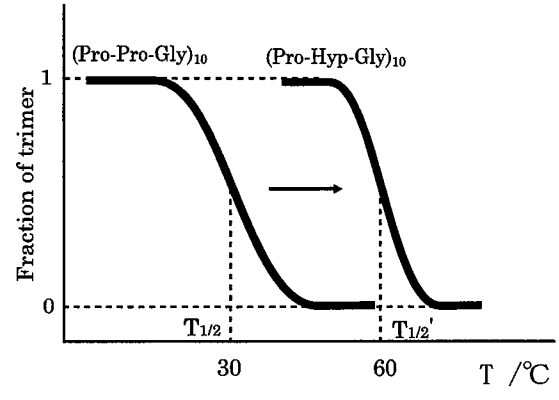

Fig. 4. Temperature dependence of trimer fraction of collagen model peptides.

ecule in solution has high molecular weight (about 300,000) and it often aggregates with each other. Then, these collagen model peptides are useful in the study, mostly study on the physico-chemical properties, of the triple helical structure of collagens.

The X-ray analysis of $(Pro\text{-}Pro\text{-}Gly)_{10}$ was first reported by Okuyama et al. They determined that the three chains of $(Pro\text{-}Pro\text{-}Gly)_{10}$, the trimer observed by sedimentation in solution by Kobayashi et al., actually forms triple helix structure [10]. In 1994 B. Brodsky et al. reported the X-ray analysis of the $(Pro\text{-}Hyp\text{-}Gly)_4(Pro\text{-}Hyp\text{-}Ala)(Pro\text{-}Hyp\text{-}Gly)_5$ peptide (Fig. 5) [11,12]. In this analysis, they proposed that this peptide also forms triple helical structure in which the water molecules make a hydrogen bonded network with neighboring water molecules and peptide chain. One of their conclusion derived from this study is that the water surrounding the triple helix stabilizes the triple helix structure of this peptide. Recently, B. Brodsky reported the refined X-ray analysis of $(Pro\text{-}Pro\text{-}Gly)_{10}$ and proposed that the water surrounding the molecule also stabilize this polytripeptide by the same mechanism as that they proposed for the $(Pro\text{-}Hyp\text{-}Gly)_4(Pro\text{-}Hyp\text{-}Ala)(Pro\text{-}Hyp\text{-}Gly)_5$ peptide [13]. A similar proposal that triple helix is stabilized by the water molecules is also reported by another group [14]. This study was obtained by IR spectroscopy of films [15]. None of these studies give any information about how these peptides are stabilized in solution even though a lot of microscopic obser-

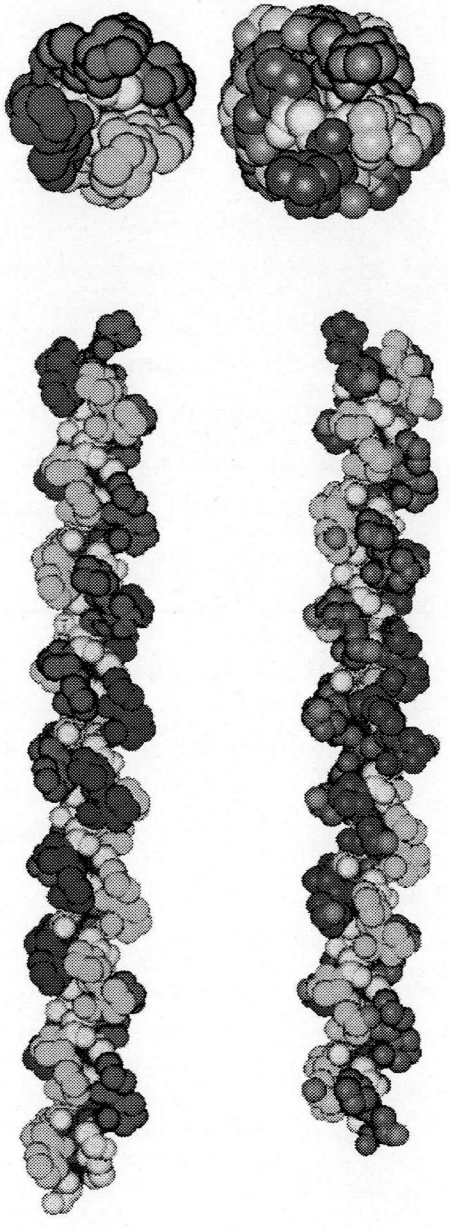

$(Pro\text{-}Pro\text{-}Gly)_{10}$ $(Pro\text{-}Hyp\text{-}Gly)_{10}{}^{*}$

Fig. 5.Crystal structures of collagen model peptides, shown (up) in a top view and (down) in a side view[11,13]. All glycine residues are shown in yellow and OH groups of $(Pro\text{-}Hyp\text{-}Gly)_{10}$ are shown in pink.

*Crystal structure of $(Pro\text{-}Hyp\text{-}Gly)_4(Pro\text{-}Hyp\text{-}Ala)(Pro\text{-}Hyp\text{-}Gly)_5$.

vations using ORD, CD and NMR spectroscopy have already been done [15-20]. In additions, theoretical analyses of the mechanism of the forming triple helix structure have also been made [21-23]. Owing to the lack of sufficient information on macroscopic quantities of the transition of these polypeptides, the mechanism of stabilization of triple helix structure in solution is still not known.

The author studied collagen model peptides in solutions, in order to deduce the mechanism of transition in solution, especially on formation of trimer (three stranded triple helix) and on transition of the three stranded triple helix to a single chains in solution by using various detailed physico-chemical methods systematically. The author studied both $(ProProGly)_{10}$ and $(Pro\text{-}Hyp\text{-}Gly)_{10}$, and also $(Pro\text{-}Pro\text{-}Gly)_5$ and $(Pro\text{-}Hyp\text{-}Gly)_5$ which all exist in solution as single chains at room temperature, thereby expecting to obtain information on the single chains in solution. Sedimentation analysis, differential scanning calorimetry and densitometry of the solution were performed to clarify the macroscopic properties. From a microscopic point of view, the circular dichroism and ultra violet spectroscopy as well as nuclear magnetic resonance spectroscopy were made.

In Chapter I, the author provides a thermodynamic interpretation of the transition from the three stranded triple helix to a single chain for the collagen model peptides and suggests that the transition can be understood as a phase transition. In chapter II, the author estimates the thermodynamic quantities of the transition from the three stranded triple helix to single chains for the collagen model peptides. In chapter III, the author describes the NMR studies of the transition of collagen model peptides. New transition at a lower temperature was observed. This transition depicts a transition of a triple helix at low temperature to a triple helix at higher temperature before the transition to single chains. In Chapter IV, the transition from the three stranded triple helix to single chains is found experimentally, in the first time, to accompany by discrete increases in the partial molar volume which is important to interpreting the nature of the transition.

Chapter I

Phase transition of collagen model peptides observed by microcalorimetry

I-1 Introduction

In the last four decades, many experimental [17,18,24-26] and theoretical [27-32] studies have been made on the transition of proteins in solution. Most of these works have focused on the transition of the proteins under equilibrium conditions or on the processes to attain equilibrium states. Studies of non-stationary states [33-35] should equally be important, because the system of interest often exists as a non-stationary states, but the lack of experimental evidence has so far limited a detailed discussion on the physical significance of the transition dynamics in non-stationary states.

In this chapter, the author has investigated the non-stationary states observed in the transition of the sequenced polytripeptides, $(Pro\text{-}Pro\text{-}Gly)_{10}$ and $(Pro\text{-}Hyp\text{-}Gly)_{10}$, as a model of fibrous protein by two complementary methods: microcalorimetry and ultraviolet (UV) absorption spectrometry.

To investigate non-stationary states, thermal transitions of these sequenced polytripeptides were measured by a Privalov type microcalorimeter together with an UV spectrometer at various scanning rates in temperature.

We have observed a shift of peaks caused by changing in the scanning rates in the C_p-temperature measurements on the transition of the polytripeptides. The observation of a distinguished peak shift in microcalorimetry is of special importance, because it is indicative of a general extension of the definition of the first-order phase transition.

I-2 Experimental

Sample preparations

The samples of $(Pro\text{-}Pro\text{-}Gly)_{10}$ and $(Pro\text{-}Hyp\text{-}Gly)_{10}$ synthesized by the Merrifield methods were purchased from Peptide Institute Inc., Japan. These samples were first dissolved in hot water at 80°C. After keeping the solution for 1 hour at this temperature, the solution was gradually cooled in a room at 22°C and then kept at 10 °C for further measurements. The concentration of each solution was determined by precise amino acid analysis.

Differential scanning calorimetric (DSC) measurements

A Privalov type adiabatic differential scanning microcalorimeter (DASM-

4M) [36,37] was used to determine the excess heat capacity at constant pressure, C_p. An active compensation without delay was achieved by controlled heating with rectangular constant-frequency impulses of regulated duration so that no calibration at each heating rate was necessary [24]. The temperature at the cell was calibrated by the boiling temperatures of ethanol and methanol.

UV absorption measurements

The temperature dependence of the UV absorption spectra of $(Pro\text{-}Pro\text{-}Gly)_{10}$ was also measured by an ultraviolet spectrometer (Shimadzu UV2200). The accuracy of the optical density measurements was ±0.001 °C. The temperature at the cell was controlled by circulating water from a programmable regulating temperature controlling bath.

I-3 Results and discussion

The reversibility of the transition was checked by performing repeated microcalorimetric scans on the same samples. An example of the results of eight consecutive scans is presented in Fig. 6. Good reproducibility and reversibility were observed for all scanning rates. No irreversible denaturation was detected. The observed transitions were endothermic, which could be described by order-disorder

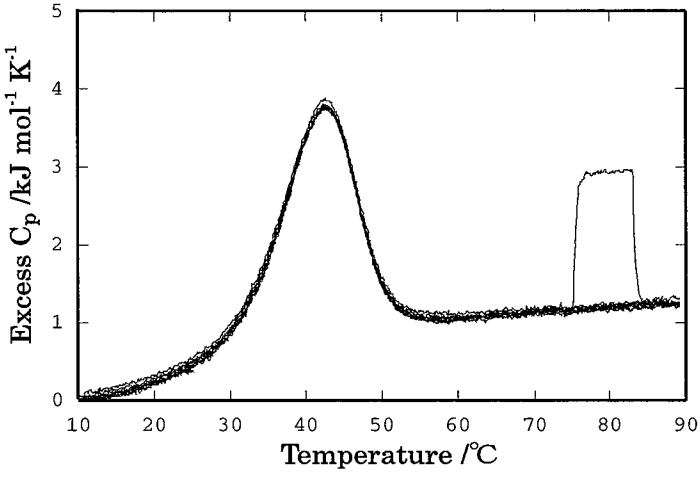

Fig. 6. Plot of eught succesive measurements of excess heat capacity of $(Pro\text{-}Pro\text{-}Gly)_{10}$ in 0.02M NaCl solution, with a peptide concentration of 0.50% and heating rate of 1K/min.

transitions accompanied by heat absorption.

As shown in Figs. 7, the excess heat capacity curves show an apparent dependence on the scanning rates. The peaks of the thermal transitions shifted to higher

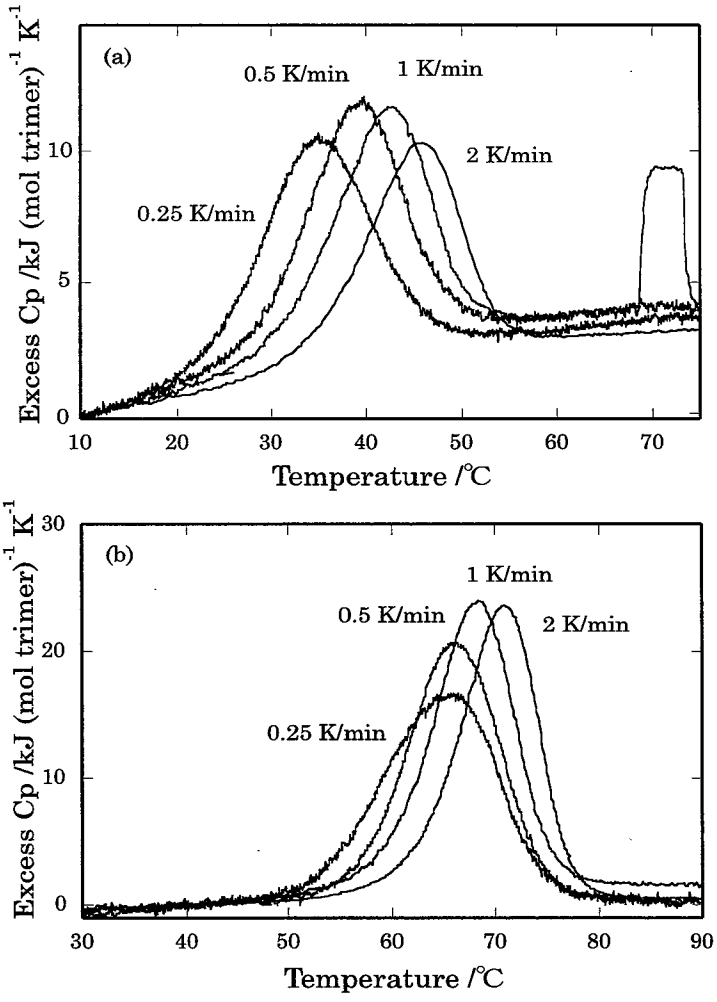

Fig.7. Excess C_p curves at a different heating rate for (a) $(Pro\text{-}Pro\text{-}Gly)_{10}$ in 0.02M of NaCl solution, with a peptide concentration of 0.54% and (b)$(Pro\text{-}Hyp\text{-}Gly)_{10}$ in 0.5% (83mM) acetic acid solu tion at a peptide cencentration of 0.50%.

temperatures as the scanning rate increases without significant changes in the shape of the curves. The shift of the transition peaks was completely reproducible. If this shift is related to delays in the response of the system caused by relaxation, the curve should also be broadened. Since the observed C*p* curve is not broadened, the excess heat capacity curve cannot be ascribed to the delay process caused by relaxation. At a high scanning rate, no heat absorption was observed even when the temperature exceeded the equilibrium transition temperature. This indicates that the thermodynamic state of the sample before the transition is maintained above the transition temperature, because a reaction or diffusion process requires heat absorption such as the latent heat. Accordingly, this observation of the peak shift suggests the presence of superheated state in the system.

The UV absorption profiles of the $(Pro\text{-}Pro\text{-}Gly)_{10}$ solutions have changed with the increases in temperature (Fig. 8.(a)). The optical density of the solution

increased with increasing of temperature, which corresponds to the increase in molecules in statistical coil states. In the transition from the triple helix to statistical coil states an order-disorder transition takes place in the system, as confirmed by the sedimentation equilibrium for $(Pro\text{-}Pro\text{-}Gly)_{10}$ in solution [7].

We made experiments on $(Pro\text{-}Pro\text{-}Gly)_{10}$ at increasing or decreasing temperature as well as at equilibrium (with intervals of 5°C). In Fig. 8(b), the system is shown to have become supercooled as well as superheated. The peaks and widths of the transition temperature observed in the UV absorption spectra in Fig. 8c are both consistent with those of the thermal analysis on $(Pro\text{-}Pro\text{-}Gly)_{10}$ at each scanning rate.

The generally accepted definition of a first-order phase transition is that the first derivatives of the Gibbs free energy of the system in question changes discontinuously at the transition temperature, so that a singularity appears in the heat capacity, as shown schematically in Fig. 9(a). The transition is an order-to-disorder transition, in which the entropy of the system increases discontinuously at the transition temperature. The appearance of the supercooled or superheated states, due to the existence of a metastable low- or high-temperature phase, is also characteristic of a first-order phase transition.

A transition without a singularity in the heat capacity curve can be included in the first-order phase transition, in a broader sense, when the following two conditions are proved experimentally: (a) the crossing of the free energy curves of two phases and (b) the existence of heat absorption ascribed to the entropy increase due to an order-disorder transition. Condition (a) can be proved experimentally by showing the existence of the superheated or supercooled states in a system.

The thermal transitions of $(Pro\text{-}Pro\text{-}Gly)_{10}$ and $(Pro\text{-}Hyp\text{-}Gly)_{10}$ have shown peak shifts that correspond to superheated and supercooled states. Furthermore, heat absorption has been observed in the transition, indicating the presence of an order-disorder transition [7]. Thus these transitions can be considered as a first-order phase transition. However, the absence of singularity in the observed thermal curves in this first-order phase transition remains to be discussed. The Gibbs free energy curves of the two phases usually cross each other at the transition temperature. The singularity disappears when there is an interaction among coexisting phases in a heterogeneous system. A typical example is a system of a limited number of particles. Because of thermal fluctuations in such a system, no singularity appears in the heat capacity curves even when the system undergoes a first-order phase transition.

Likewise, a protein solution constitutes a homogeneous phase in which native and denatured molecules interact with each other. If a low temperature "phase"

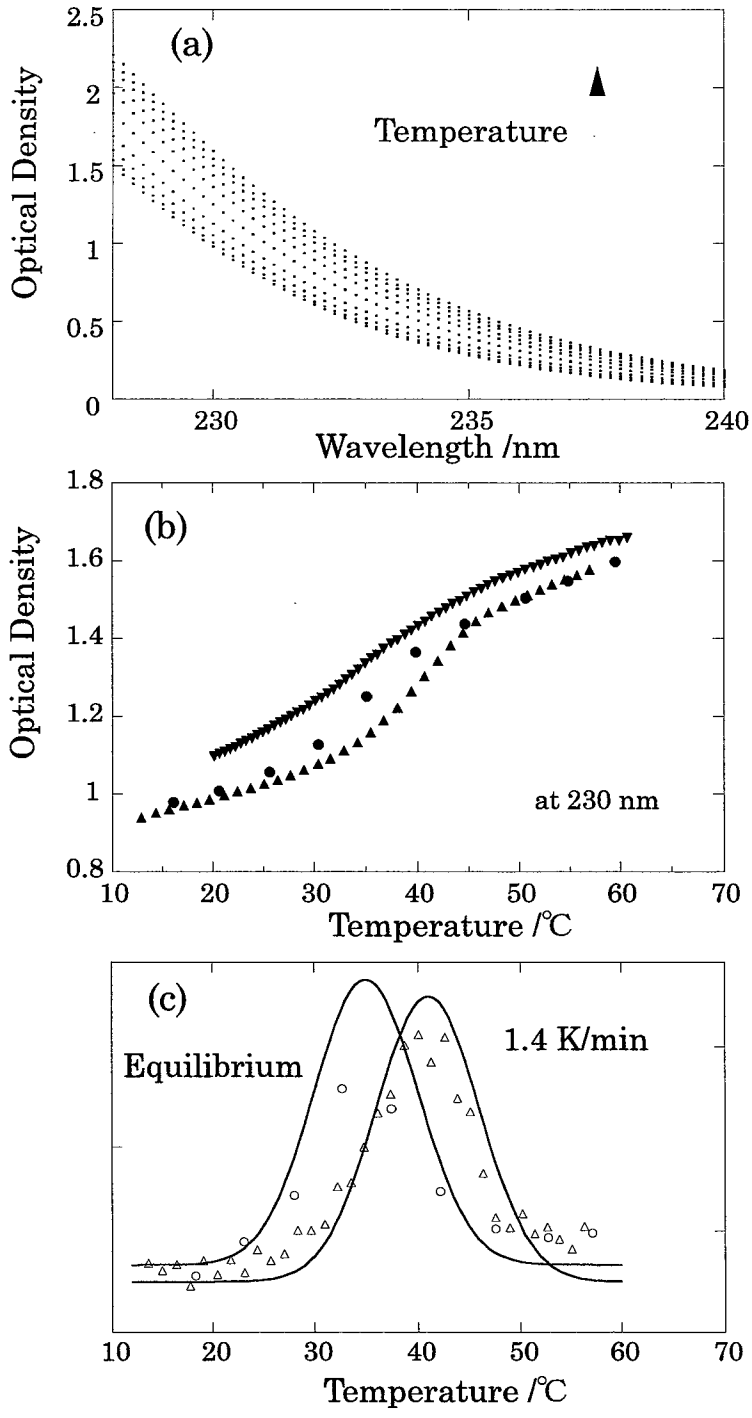

Fig. 8. UV absorption spectra of $(Pro\text{-}Pro\text{-}Gly)_{10}$ in 0.02M NaCl solutions at a peptide concentration of 0.54% at various temperature; from bottom upwards, 16.0, 20.0, 25.6, 30.4, 35.1, 39.8, 44.6, 51.5, 59.5 ℃, (b) temperature dependence of the optical density at 230 nm; ▲ heating at 1.4 K/min; ▼cooling at 0.65 K/min; ● heating with 5 ℃intervals, measured at 30 min after reaching each temperature and (c) temperature derivatives of the optical density in arbitrary units; △ heating at 1.4 K/min; ○ heating with 5 ℃intervals. The solid lines represent C_P curves.

where molecules are dominantly in the native state, coexists with that of a high-temperature 'phase' where molecules consist dominantly of denatured molecules, the no singularity can be observed at the transition temperature because of the interaction between these two phase. In other words, in a heterogeneous system consisting of s single component, the allowed degree of freedom is zero (at constant pressure) at the transition point by the Gibbs phase rule. As a result, the temperature cannot be changed as long as a heterogeneous phase exists. Accordingly, the heat capacity shows a singularity at the transition point. On the contrary, in a protein solution the system always stays as a homogeneous phase even at the transition temperature, and thus no singularity should be observed. Since the native and denatured states are in the state of thermal equilibrium, the Gibbs free energy curves of the two 'phases' should be equal at the transition temperature. This is schematically shown in Fig. 9(b). The native and denatured states in the low- and high- temperature 'phases' coexist in thermal equilibrium with a different relative

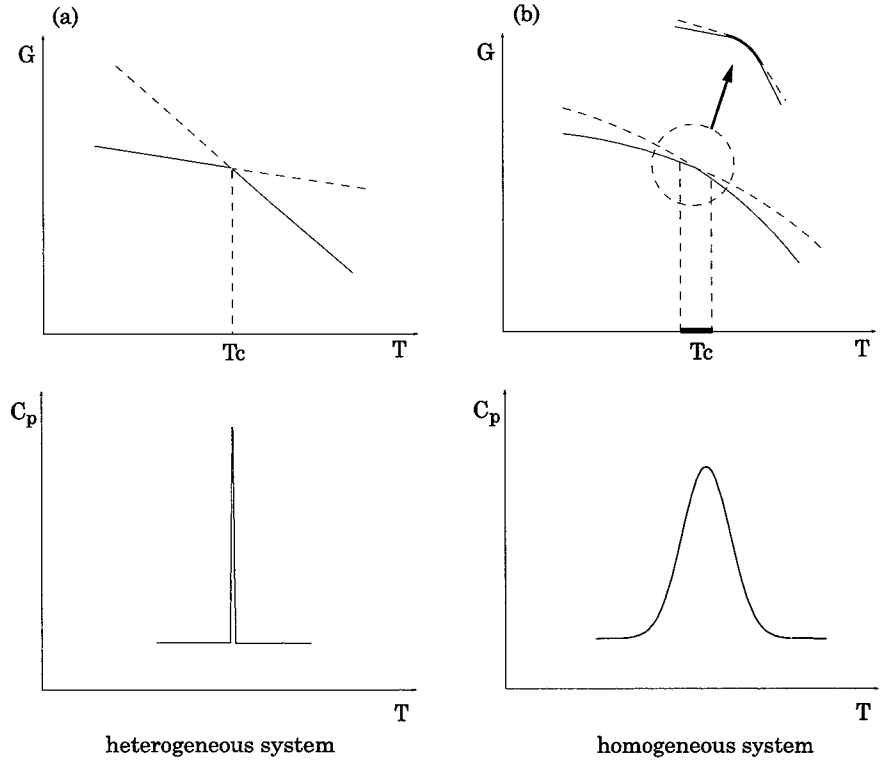

Fig. 9. (a) Gibbs free energy curves and corresponding excess heat capacity curves of a system (schematic) of a typical phase transition consisting of heterogeneous phases at transition (T_c) and (b) similar curves for a phase transition in a homogeneous phase.

abundance of molecules in these state is determined uniquely by the temperature. This explains the observed width of the transition.

Chapter II

Measurement of thermodynamic quantities of thermal transitions of collagen model peptides

II-1 Introduction

Thermal transitions of collagen model peptides, $(Pro\text{-}Pro\text{-}Gly)_{10}$ and $(Pro\text{-}Hyp\text{-}Gly)_{10}$ these peptides show a sharp transition peak unlike all the other synthetic polypeptides [38].

Nevertheless, no extensive study has yet been made using calorimetry on the thermal transition of these polytripeptides [9,16]. Calorimetry is, undoubtedly, the only method by which thermal changes of a solution as a whole can be investigated. The heat detected by calorimetry is ascribed to the partial specific heat capacity of solutes or solvents, both related to the solvent-solute interactions. For simplicity, spectroscopic methods are often chosen as tools to investigate transition temperature changes in enthalpy and entropy. Such information based on microscopic states of a molecule undergoing transition is related indirectly to the thermal transition.

In previous studies including those by spectrometry, the enthalpy or entropy changes were never evaluated under the same solvent conditions nor were the studies made systematically. In addition, the purity of the samples or the solution systems often differed so much that no critical comparisons could be made.

In chapter I, the author observed a distinct shift in peaks which we ascribed to a change in the heating rate in the rate-dependent heat capacity (C_p) measurements on the transitions of sequenced polytripeptides, $(Pro\text{-}Pro\text{-}Gly)_{10}$ and $(Pro\text{-}Hyp\text{-}Gly)_{10}$. This finding indicated of the first-order phase transition.

In this chapter, the author have investigated the dependence of thermodynamic behaviors of $(Pro\text{-}Pro\text{-}Gly)_{10}$ and $(Pro\text{-}Hyp\text{-}Gly)_{10}$ on the heating rate using microcalorimetry, ultraviolet (UV) absorption spectroscopy and circular dichroism (CD) spectroscopy. The author have obtained the equilibrium thermodynamic quantities of transitions, transition temperatures (Teq), enthalpy changes (ΔH) and entropy changes (ΔS), in various solution. The observed linear relationship between the enthalpy and entropy changes is discussed, using our previous extended definition of the first-order phase transition, as a transition of the solution from a system rich in triple helix to that rich in statistical coil.

II-2 Experimental

Sample preparations

The samples of $(Pro\text{-}Pro\text{-}Gly)_{10}$ and $(Pro\text{-}Hyp\text{-}Gly)_{10}$ were dissolved in water and dialyzed in Spectra/Pore CE dialysis tubing with a molecular weight cut off of 100 against deionized water (0.2 mS) for four days at 4 °C. After equilibration with the water, the samples were freeze dried before use. The purity of the samples was greater than 98 % by using reverse-phase high performance liquid chromatography on a Nakarai C-18 column. The solutions of polytripeptides were then prepared as described in chapter I. The concentration of the solutions is 0.5 % (2 mM polytripeptide concentration) for each experiment unless otherwise indicated.

Differential scanning calorimetric (DSC) measurements

Differential scanning calorimetry (DSC) experiments were performed with a Privalov-type adiabatic differential scanning microcalorimeter (DASM-4M). The operational cell volume was 514 μl determined by the methods proposed by Privalov [39-41]. The DSC experiments were performed at heating rates of 0.25, 0.5, 1 and 2 K/min.

UV absorption and Circular dichroism measurements

The heating rate dependence of the UV absorption spectra at 230 nm of $(Pro\text{-}Pro\text{-}Gly)_{10}$ was recorded on a Shimadzu double beam UV spectrometer controlling the temperature by circulating water. The heating rate dependence of the residual molar ellipticity at 227 nm was recorded on a Jasco Model J720 CD spectrometer equipped with a programmable Peltier thermoelectric temperature controller. For CD measurements, ellipticity of the solution was measured at heating rates of 0.1, 0.25, 0.5, 1 and 2 K/min as well as at equilibrium condition. For the equilibrium experiment, the temperature in the cell was increased at a rate of 0.1 K/min and equilibrating for 20 min at each temperature before collecting data. Data were recorded at every 5° C. Both for the CD and UV experiments, the pathlength of the cell was 1 mm .

II-3 Results and discussion

Heating rate dependence of the transition temperatures

The C_p curves of $(Pro\text{-}Pro\text{-}Gly)_{10}$ and $(Pro\text{-}Hyp\text{-}Gly)_{10}$ showed a distinct dependence on the heating rate as shown in Fig.10 for $(Pro\text{-}Pro\text{-}Gly)_{10}$. The peak of the thermal transition shifted to higher temperature as the heating rate was increased. The

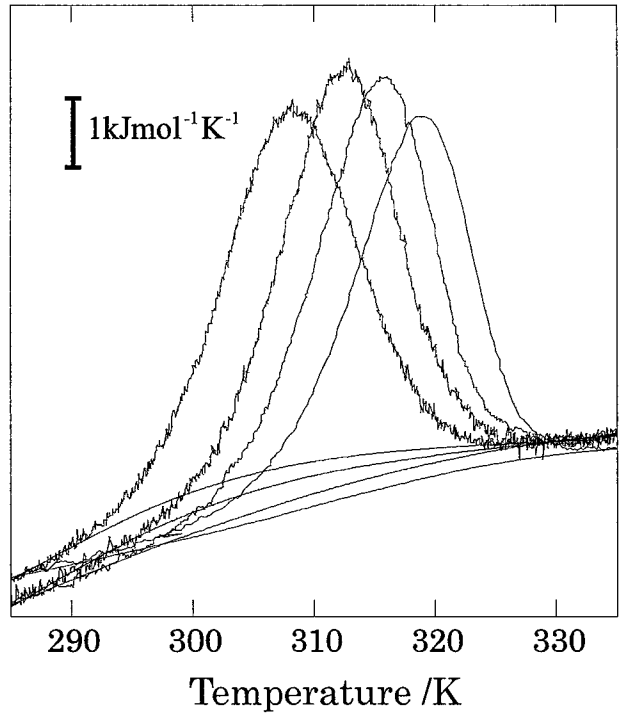

Fig. 10. Apparent excess heat capacity of $(Pro\text{-}Pro\text{-}Gly)_{10}$ at different heating rates. Experiments were performed in 20mM sodium chrolide. Heating rates are from left to right 0.25, 0.5, 1 and 2 K/min.

transition temperatures of solutions with the same apparent composition condition are different from those previously obtained using samples without dialysis against deionized water. This is not unreasonable since small amounts of residuals should change the two Gibbs free energies, which correspond to the solution before and after transition. The transition temperature of a system is expected to correspond to the crossing temperature of these two Gibbs free energies and be changed by the addition of a small amount of molecules.

Thermal curves are shown with baselines in Fig. 10. The heat capacities in the high temperature regions after transition were found to depend sparingly on temperature for all solutions measured, as in protein solutions. In contrast, in the region before the transition a distinct linear dependence on temperature of apparent heat capacities were observed in each solution, unlike those generally observed in protein solutions. The dCp/dT before the transition was found to increase with a decrease in the heating rate for all solutions measured. It is thus anticipated that in an equilibrium condition this dependence is more distinct.

The excess heat capacity curve after correction for the baseline was employed in the estimation of the transition enthalpy. The baseline was drawn by interpolating two Cp curves before and after the transition, as is usually performed in the calorimetry of systems undergoing phase transitions

The dependencies of the peaks of the thermal transitions in various solutions are plotted in Fig. 11, against the heating rate for the $(Pro\text{-}Pro\text{-}Gly)_{10}$ and $(Pro\text{-}Hyp\text{-}Gly)_{10}$ solutions. The equilibrium transition temperature (defined as the temperature for a maximum differential increment of the observed quantity) has been evaluated using CD and UV spectroscopy for $(Pro\text{-}Pro\text{-}Gly)_{10}$ at various heating rates, as shown. The dependence on the heating rate (r) of the peaks of the thermal transition (T_r) was found to be described by the following equation irrespective of the solution condition including those diluted (0.083% polytripeptide concentration):

$$T_{eq} = T_r + 14.96 \log [(r_o + 0.38)/(r + 0.38)] \qquad \text{(Eq. 1)}$$

where r_0 is zero (an equilibrium experiment) and T_{eq} is the transition temperature at a zero heating rate corresponding to the equilibrium transition temperature. The difference in the dependence of $(Pro\text{-}Pro\text{-}Gly)_{10}$ and $(Pro\text{-}Hyp\text{-}Gly)_{10}$ on the heating rate was found to be insignificant.

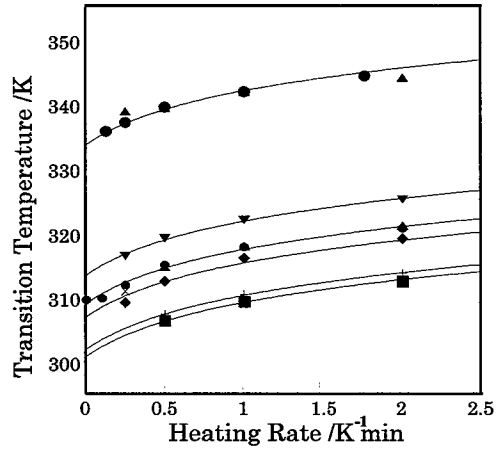

Fig. 11. Heating rate dependence of transition temperature for $(Pro\text{-}Pro\text{-}Gly)_{10}$ and $(Pro\text{-}Hyp\text{-}Gly)_{10}$ at several solutions: Tr of (Pro-Pro-Gly)10 from DSC experiments (■) in water; (◆) in 20 mM sodium chloride solution; (▲) in 83 mM acetic acid solution; (▼) in 83 mM deuterated acetic acid/D2O, Tr of $(Pro\text{-}Pro\text{-}Gly)_{10}$ in 50 mM acetic acid from CD experiments (●), Tr of $(Pro\text{-}Pro\text{-}Gly)_{10}$ in 50 mM acetic acid from UV experiments (×) and Tr of (Pro-Hyp-Gly) from DSC experiments (o) in 500 mM acetic acid; (△) in 83 mM acetic acid. Experiments were performed with polytripeptide concentration of 2 mM excepted for the solution of (Pro-Pro-Gly)10 at 0.083 mM in water (+).

Determination of the equilibrium thermodynamic quantities of the transition

The author has calculated from the apparent excess C_p curve the heat needed to induce the transition of the solution at each heating rate (*ΔHr*). The obtained *ΔHr* are plotted against the heating rates in Fig.12. This clearly illustrates that *ΔHr* is independent of heating rate. The equilibrium enthalpy change *(ΔH)* of the transition could be obtained irrespective of the heating rate. We have thus succeeded in evaluating the enthalpy changes *(ΔH)* for the thermal transition of $(Pro\text{-}Pro\text{-}Gly)_{10}$ and $(Pro\text{-}Hyp\text{-}Gly)_{10}$ solutions.

The entropy change of the solution *(ΔS)* have been evaluated from the equation $\Delta S=\Delta H/T_{eq}$. The equilibrium thermodynamic quantities, can therefore be obtained from a single calorimetric measurement at a certain heating rate in these systems. We have thus been able to evaluate the equilibrium thermodynamic quan-

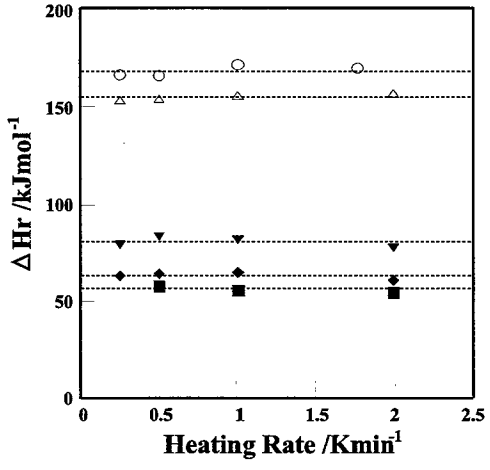

Fig. 12. Enthalpy changes from DSC experiments for $(Pro\text{-}Pro\text{-}Gly)_{10}$ and $(Pro\text{-}Hyp\text{-}Gly)_{10}$ at different heating rates: (Δ) Hr of $(Pro\text{-}Pro\text{-}Gly)_{10}$ (■) in water; (◆) in 20 mM sodium chloride solution; (▼) in 83 mM deuterated acetic acid/D_2O solution and Δ Hr of $(Pro\text{-}Hyp\text{-}Gly)_{10}$ (○) in 500 mM acetic acid; (△) in 83 mM acetic acid.

tities of the transition from DSC measurements in these systems. The measured DSC data in various solutions of $(Pro\text{-}Pro\text{-}Gly)_{10}$ and $(Pro\text{-}Hyp\text{-}Gly)_{10}$ are shown in Table I. These data indicate remarkable change in transition temperatures, enthalpy and entropy changes of the transition which depend on the solvent conditions. The transition temperature of proteins may also depend significantly, for example, on the choice of the buffer solutions. These results indicate that the sys-

Table I Themodynamic quantities[a] of $(Pro\text{-}Pro\text{-}Gly)_{10}$ and $(Pro\text{-}Hyp\text{-}Gly)_{10}$

Peptide	Solvent		Tm /C	ΔH /kJmol^{-1}	ΔS /Jmol^{-1}K^{-1}
$(Pro\text{-}Pro\text{-}Gly)_{10}$	Water		27.7	55.7	185
			28.7[b]		
	NaCl /mM	50	29.8	65.4	216
		100	31.2	69.3	228
		200	32.2	68.7	224
		500	33.6	76.8	250
	AceticAcid /mM	5	33.7	73.4	239
		10	34.3	81.9	266
		20	35.1	74.9	243
		50	35.8	78.3	253
		500	36.1	87.4	283
	Deuterium Oxiside				
	CD_3COOD /mM	83	40.5	81.9	261
$(Pro\text{-}Hyp\text{-}Gly)_{10}$					
	Acetic Acid /mM	83	60.1	156.3	469
		500	60.4	172.2	516

[a] Obtained from the second run using the same solution without refilling the cell after confirmation of the high reproducibility of the measurements. [b] Peptide concentration: 0.083% (0.33mM)

tematic changes of solvent compositions are indispensable, especially in the investigations of $(Pro\text{-}Pro\text{-}Gly)_{10}$ and $(Pro\text{-}Hyp\text{-}Gly)_{10}$ systems.

Linear relationship between enthalpy change and entropy changes of the transition

Fig. 13 shows plots of the evaluated enthalpy changes versus entropy changes of the thermal transition of $(Pro\text{-}Pro\text{-}Gly)_{10}$ and $(Pro\text{-}Hyp\text{-}Gly)_{10}$ in various solution obtained by DSC measurements. They show a linear relationship, indicating an enthalpy-entropy compensation [41,42]. All the available data found in literature obtained by methods other than calorimetry are also shown. They deviate appreciably from the linear relationship found for the calorimetric data.

The phenomenon of compensation is often proposed as a diagnostic test for the participation of water in the process considered [42]. The transition of $(Pro\text{-}Pro\text{-}Gly)_{10}$ and $(Pro\text{-}Hyp\text{-}Gly)_{10}$ may be accompanied by the volume changes, which induce changes in the surface areas of the molecule. With changes in the solvent, the surface areas will be changed and, accordingly, the Gibbs free energy of the system will be changed. The enthalpy- entropy compensation would then be fulfilled in theory when the enthalpy and entropy changes per unit surface area are identical.

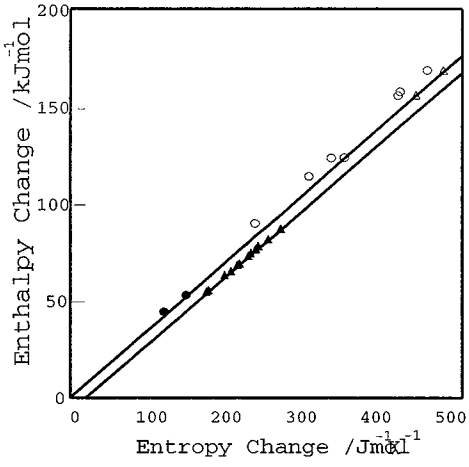

Fig. 13. Plot of enthalpy changes versus entropy changes: (●) $(Pro\text{-}Pro\text{-}Gly)_{10}$; (○) $(Pro\text{-}Hyp\text{-}Gly)_{10}$ from DSC experiments and (▲) $(Pro\text{-}Pro\text{-}Gly)_{10}$; (△) $(Pro\text{-}Hyp\text{-}Gly)_{10}$ from the other experiments than calorimetry. The straight lines were fitted to the experimental points obtained from DSC measurements by linear regression.

Relation to the extended phase transition

In a previous chapter we described the transition of $(Pro\text{-}Pro\text{-}Gly)_{10}$ and $(Pro\text{-}Hyp\text{-}Gly)_{10}$ as endothermic, which could be described by order-disorder phase transitions accompanied by heat absorption. Enthalpy-entropy compensation is normally considered to be observed when a reaction consists of a single process [42]. The thermal transition of $(Pro\text{-}Pro\text{-}Gly)_{10}$ and $(Pro\text{-}Hyp\text{-}Gly)_{10}$, on the microscopic level, consists of multiple-processes. The existence of the compensation phenomena in the transition, however, seems to suggest that the cause of the Gibbs free energy difference between two solutions arises mainly from the difference in the way water participates in the construction of conformations of molecules in each solution. The transition is thus considered as a macroscopic process, which could be described as an extended first-order phase transition.

Chapter III

NMR observation of the thermal transition of $(Pro\text{-}Pro\text{-}Gly)_{10}$

III-1 Introduction

Spatial structure determinations of ordered states in solution using NMR techniques have now become common procedure in the investigation of biopolymers. For small proteins and peptides, one can determine the structure of a specific active site in a molecule [43]. Studies of the denatured states of proteins induced by urea, acids and alcohols and induced by elevation of temperature have recently been made, by which the relevance of the residual structure in the denatured states of proteins to the mechanism of protein folding have been investigated [44]. Studies of transitions by NMR should be equally important, but the lack of experimental evidence indicating the coexistence of natured and denatured states of proteins in solution has so far limited the discussion on the microscopic changes of molecules accompanied by thermal transition. Collagen model polypeptides, make solutions consisting of natured and denatured molecules over a wide temperature range.

The thermal transition of $(Pro\text{-}Pro\text{-}Gly)_n$ (n=10.15) was first studied using NMR by Kobayashi and Kyogoku [45]. The thermal transition of collagen model polytripeptides has recently been studied by NMR [17, 46], but no detailed analysis of the thermal transition has yet been reported based on the assignments of the NMR spectra at each temperature.

In this chapter, the author investigated the transitions of $(Pro\text{-}Pro\text{-}Gly)_{10}$ by observing the ^1H and ^{13}C-NMR spectra. The results provide evidence for the existence of the structural changes in the triple helix at low temperature, before the start of a drastic transition of the triple helix to the statistical coil. The relationship between results obtained by NMR and those by microcalorimetry is also discussed

III-2 Experimental

Sample preparations

The samples of $(Pro\text{-}Pro\text{-}Gly)_{10}$ were repeatedly freeze-dried and finally redissolved in 0.5% (85mM) CD_3COOD-D_2O solution using 99.96% deuterated CD_3COOD and D_2O. In the DQF COSY experiment, 1.5% (6mM) $(Pro\text{-}Pro\text{-}Gly)_{10}$ solution was used. Saturated $(Pro\text{-}Pro\text{-}Gly)_{10}$ solutions were used in all other experiments.

The chemical shifts of HDO and the methyl signal of CD_3COOD at each tem-

perature in ^{1}H and ^{13}C spectra were determined by 3-(trimethyl-silyl)-1-propanesulfonic acid (DSS). The chemical shifts in the NMR spectra were calibrated using these values.

NMR measurements

All the NMR measurements were made using a JEOL JNM-A600 spectrometer; ^{1}H and ^{13}C -NMR measurements were carried out at 600 MHz and at 150 MHz, respectively.

Assignments were made using two-dimensional phase-sensitive double quantum filtered correlation spectroscopy (DQF COSY) [47], heteronuclear multiple quantum coherence spectroscopy (HMQC) using gradients [48] and rotating frame Overhauser effect spectroscopy (ROESY) measurements [49].

The excess heat capacity at constant pressure C_p, of the D_2O solution was measured using a Privalov-type adiabatic differential scanning microcalorimeter (DASM-4M).

III-3 Results and discussion

Assignments of ^{1}H and ^{13}C-NMR spectra of $(Pro\text{-}Pro\text{-}Gly)_{10}$

The DQF-COSY (10 °C) and HMQC (70 °C) spectra are shown in Fig. 14(a) and 14(b), respectively. The cross peaks in the DQF-COSY spectrum represent

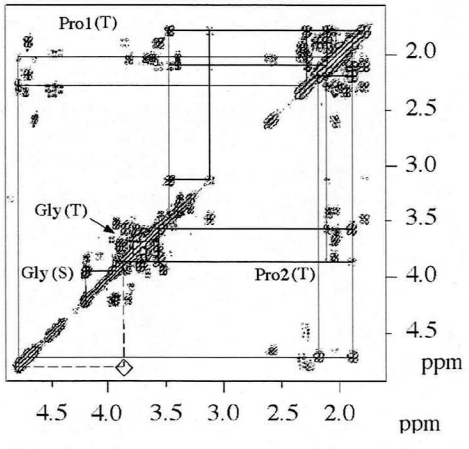

Fig. 14(a) Two-dimensional NMR spectra of $(Pro\text{-}Pro\text{-}Gly)_{10}$: DQF-COSY spectrum at 10 ° C. The solid lines connect the cross peaks assigned to Pro1 (upper part), Pro2 (lower part), and Gly. T and S represent the triple helix and the statistical coil, respectively. The interchain NOE cross peak between the CαH of Pro1 and the CdH of Pro2 observed in the ROESY spectrum appears at a position indicated by (◇). Unspeci fied cross peaks are assigned to terminal ends or to impurities.

the existing ^{1}H-^{1}H J- couplings of the nuclear spins in the system [47]. Each cross peak in the HMQC spectrum is derived from the correlation of the protons and carbons that are directly bonded [49].

After assignments of ^{1}H spectra have been made, the ^{13}C spectra can be assigned by HMQC spectra. In Fig. 14(b), some cross peaks assigned to cis isomer are indicated.

Kobayashi et al. [50] had prepared (Pro-Pro(d)-Gly)$_{10}$ in which the CαH of the second proline (Pro2) in the tripeptide unit was substituted by deuterium. The d-substituted proline as a starting material was obtained by the racemization process in deuterium oxide accelerated with high pH and high pressure following the separation of stereoisomer by the L-leucyl-dipeptide method [51].

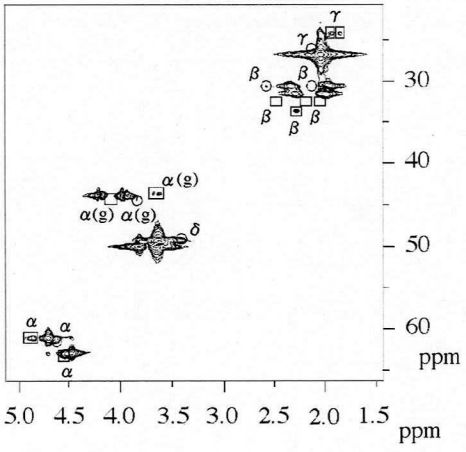

Fig. 14-(b) Two-dimensional NMR spectra of (Pro-Pro-Gly)$_{10}$; HMQC spectrum at 70 ° C: (○) positions of the cross peaks of the terminal end; (□) the cis conformer. Marks α–δ represent cross peaks related to protons in proline, while α(g) denotes the α resonances of glycines.

The ^{1}H-NMR spectra observed at 75 °C are shown in Fig. 15(a). The assignments of the ^{1}H and ^{13}C -NMR spectra at 10, 40, and 70 °C are shown in Fig.15 (b) and Fig.16, respectively. By a comparison of the ^{1}H spectra of both samples with and without deuterium substitution, the author ascribed the peak at 4.6 ppm to the CαH of the first proline (Pro1) and 4.4 ppm to CαH of Pro2 in statistical coil. Other protons in Pro1 and Pro 2 at 70 °C are then assigned by the DQF-COSY spectrum. The CαH for Gly is distinguished as a distinct nondegenerate cross peak. Based on the assignments of the ^{1}H spectrum, the ^{13}C spectrum is assigned by the HMQC spectrum. The assignments of the terminal groups are based on those of the ^{1}H spectra of oligopeptides [45]. Small peaks are observed in the ^{13}C spectrum at 70 °C

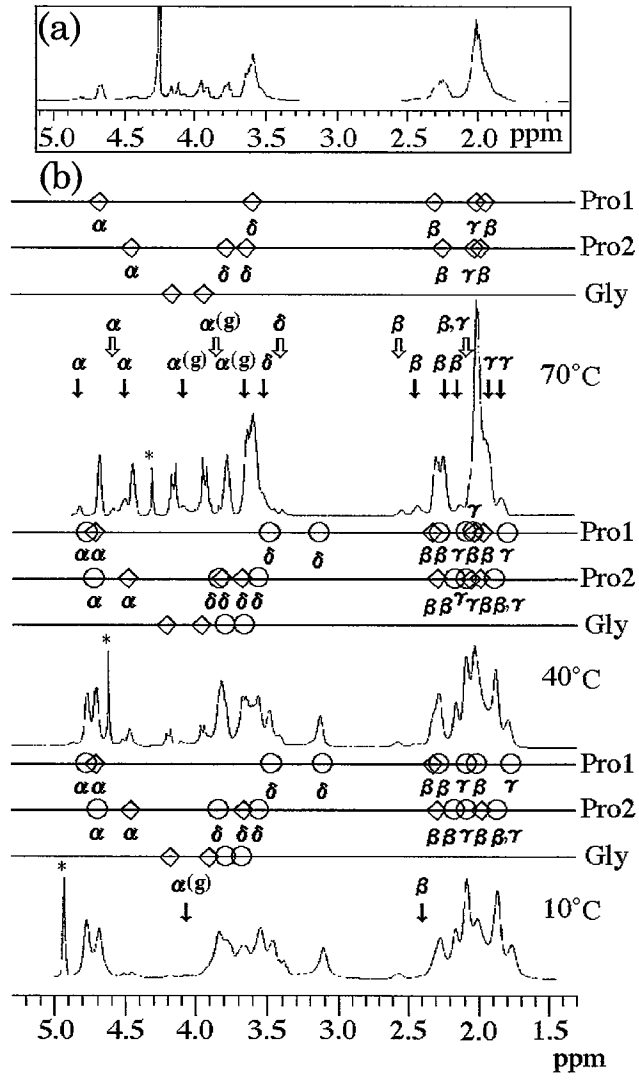

Fig. 15. (a) 1H spectrum of (Pro-Pro(d)-Gly)$_{10}$ at 75 ° C in 10% CD_3COOD-D_2O solution. (b) Assignments of the 1H spectra of (Pro-Pro-Gly)$_{10}$ at 10, 40 and 70 ° C. The assignments are indicated on the three horizontal lines and on the spectra: reso nance position (○) the triple helix; (◇) the statistical coil. See Fig. 14 for α– δ and α(g). Resonance position: (⇓) the terminal residue and (↓)the cis conformer. The peaks due to HDO are indicated by (*).

for every major peak. According to the assignments of H-Trp-(Pro)$_n$-Tyr-OH made by Poznanski et al [52], these small peaks are assigned to the carbons in residues taking the cis conformation. The cis peaks in the ^{1}H spectra are assigned using the HMQC spectrum shown in Fig. 14(b), as shown in Fig. 14.

Assignments of the spectra at 10°C are then performed similarly. The peak at4.8 ppm and 4.7 ppm are ascribed to the CαH of Pro1 and Pro2 in triple helix, respectively. Other protons are determined by the DQF-COSY spectrum. These

assignments are further confirmed by the ROESY spectrum [49] (see legend of Fig. 14(A)). The ^{13}C spectrum at 10 °C is also assigned using the HMQC spectrum.

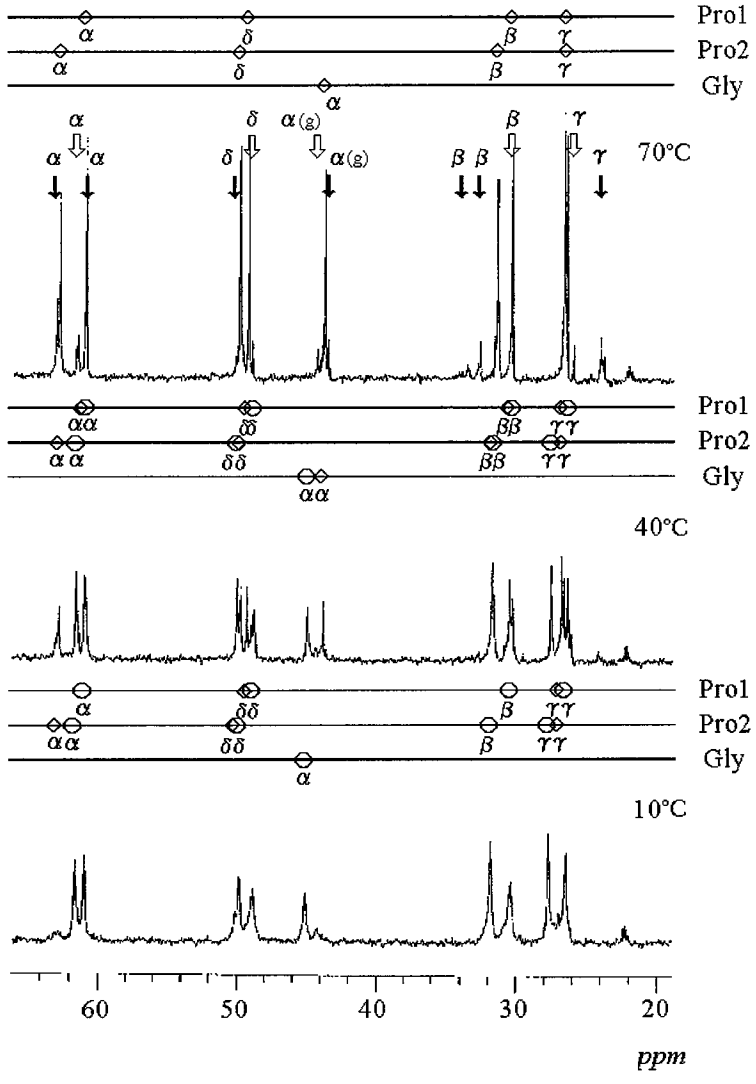

Fig. 16. Assignments of ^{13}C spectra of $(Pro\text{-}Pro\text{-}Gly)_{10}$ at 10,40,and 70 ° C. See Fig. 14 for the marks. The peak at 22 ppm is assigned to the methyl group in CD_3COOD.

The cis peaks at 10 °C are assigned by inspection of the temperature-dependent changes of the ^{1}C spectra. The existence of the resonance for the cis conformer at 10 °C can be regarded as experimental evidence for the existence of peptides in the statistical coil in solution below 10 °C. Evaluation of the area of each peak at each temperature shows that the ratio of the cis conformer in the

statistical coil is always slightly higher than 20 % and that the ratio is independent of temperature, similar to the case of proline derivative [53].

The phase transition observed by NMR spectra

Fig 17(a) shows the apparent excess heat capacity curves (C_p) of the solution of

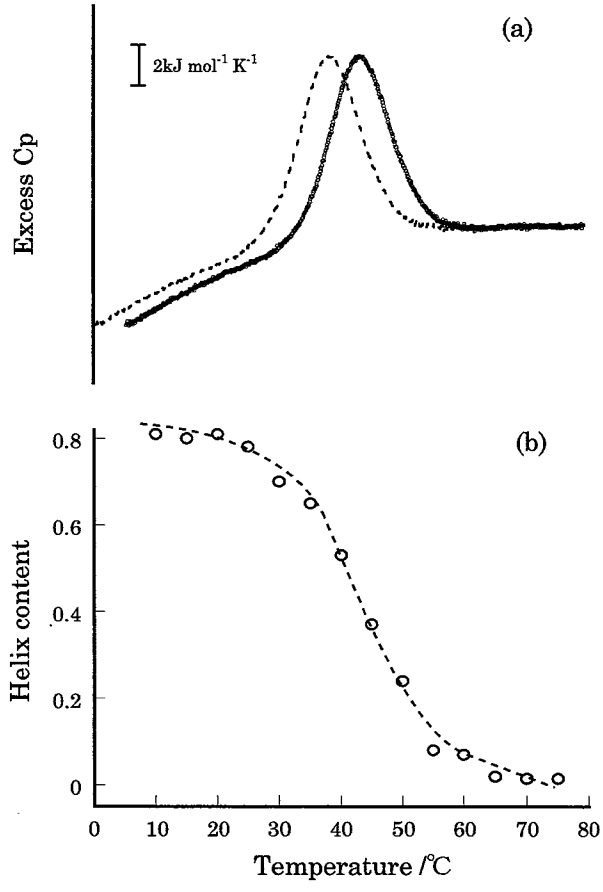

Fig. 17.(a) The solid line describes the excess C_p curve of $(Pro\text{-}Pro\text{-}Gly)_{10}$ in 0.5% CD_3COOD solution at a peptide concentration of 0.50% at 0.25 K/min. The broken line represents the shifted C_p curve corresponding to the equilibrium experiment. (b) Temperature dependence of helix content of $(Pro\text{-}Pro\text{-}Gly)_{10}$ determined by the $C_\delta H$ peak of Pro1 at 3.1 ppm in the triple helix.

$(Pro\text{-}Pro\text{-}Gly)_{10}$ at heating rate 0.25 K/min. The transition temperature corresponding to an equilibrium experiment can be calculated from the equation derived based on the dependence of the transition temperature on the heating rates (see Chap. II). The peak of the C_P curve in the Fig. 17(a) is 43 °C and the equilibrium transition temperature will be 40 °C.

. Corresponding ^1H-NMR spectra at various temperatures are shown in Fig. 17(b). Comparing to the results of NMR with those of calorimetry, the changes of

spectra accompanied transition is observed in more extended region. Actually, by observing the peak areas of $C_\delta H$ proton of Pro 1 in the triple helix at 3.1 ppm and $C_\alpha H$ proton of Gly in the statistical coil at 4.2 ppm, the transition region as observed by NMR is from 20 to 70.

Temperature dependence of ^1H chemical shifts

Fig.18 shows typical examples of the dependence of the chemical shifts of pro-

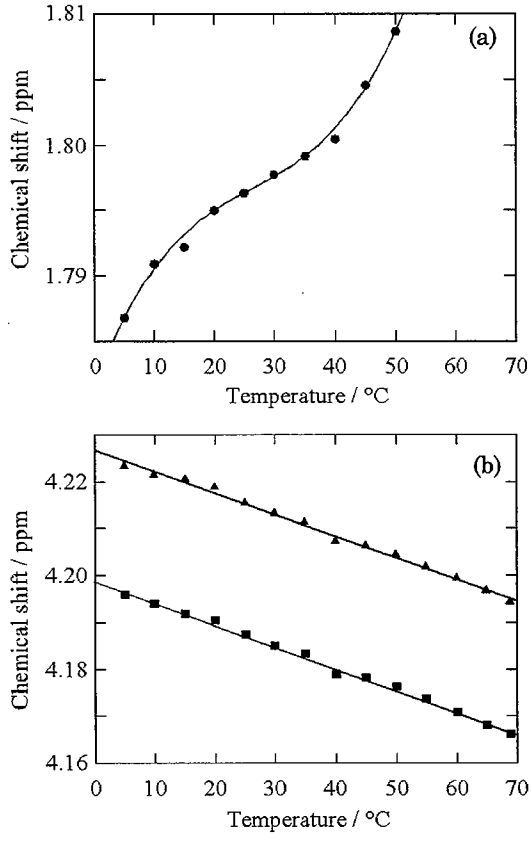

Fig. 18. Chemical shifts of $(Pro\text{-}Pro\text{-}Gly)_{10}$ are plotted versus temperature . (a) $C_\gamma H$ of Pro1 in the triple helix and (b) $C_\delta H$ of glycine in the statistical coil. Chemical shifts are expressed relative to DSS.

tons on temperature. DSS was added as an internal reference in this experiment. The transition temperature of the solution is found to shift 3 °C on the addition of DSS.

The chemical shifts of $C_\gamma H$ and $C_\delta H$ protons of Pro1 in the triple helix draw sigmoidal curves with an increase in temperature, whereas in the statistical coil they

depend linearly on temperature. Our experimental results indicate that the triple helix consists of two distinct states; one corresponds to a lower temperature state (LT) and the other to a higher temperature state (HT). They undergo a fast exchange transition with only small changes in chemical shifts of protons, about 0.015 ppm for $C_{\gamma}H$ and 0.006 ppm for $C_{\delta}H$. The chemical shifts in DNAs, where similarly fast but overall structural transitions are performed, depend on temperature with distinct changes in chemical shifts by as much as 0.55 ppm [54].
As shown in Fig. 18, the LT to HT transition takes place in the region of 10-40 °C, while the transition from triple helix to the statistical coil takes place in the region of 20-70 °C. At the transition temperature, about 40 °C from the thermal curve, all the molecules in the triple helix are considered to be in HT. The transition of the triple helix (LT) to a preparatory state of the transition (HT) is probably accompanied by an exchange in the positions of water interacting with the triple helix, because they occur without heat absorption and with small changes in the chemical shifts. The findings if this transition is important since such a preparative transition should also be found in proteins and play an important role in the kinetics.

Chapter IV

The partial molar volume of collagen model peptides

IV-1 Introduction

Partial molar volume

When a mole of solute is dissolved in a infinite amount of solvent, the volume occupied by the solute is defined as the partial molar volume of the solute as shown in Fig. 19 [55,56]. The total volume of the solution is expressed as in Eq. 2, the apparent partial molar volume of the solute, Φ_2 can be obtained from Eq.3, and the partial molar volume of the solute, V_ϕ is the value of Φ_2 at infinite dilution. In Fig. 20, the dependencies of the total volume of the solution on the amount of the solute are shown and in case 1, the partial molar volume can be obtained from the concentration dependence of the total volume at any concentration.

Because of the difficulty in the precise determination of the volume change,

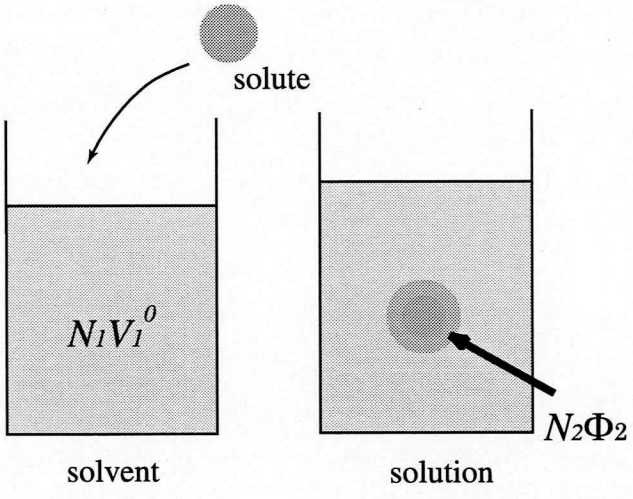

$$V = N_1 V_1^0 + N_2 \Phi_2 \qquad \text{(Eq. 2)}$$

V: total volume
N_1: amount of solvent
V_1^0: molar volume of solvent
N_2: amount of solvent
Φ_2: apparent molar volume of solute
V_ϕ: partial molar volume

$$V_\phi = \left(\frac{\partial V}{\partial N_2}\right)_{P,T,N_1} = N_2 \left(\frac{\partial \Phi_2}{\partial N_2}\right)_{P,T,N_1} + \Phi_2 \qquad \text{(Eq. 3)}$$

Fig. 19. The partial molar volume of solute in solution.

the partial molar volume of the solute can usually be obtained experimentally from the concentration dependence of the density of the solution using Eq. 4 (Fig. 20) [55].

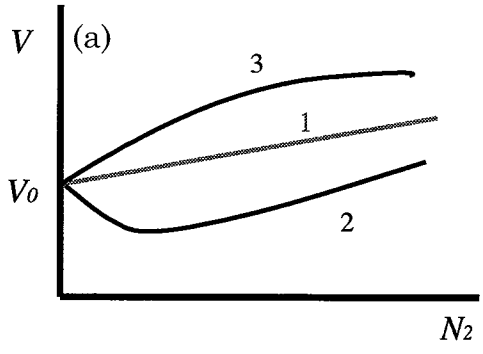

1. ideal binary
2. non-ideal (of electrolyte)
3. non-ideal (of non-polar solute)

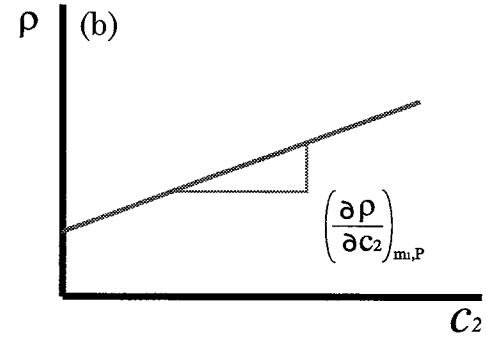

$$\left(\frac{\partial \rho}{\partial c_2}\right)_{m,P} = 1 - \bar{\nu}\rho^{\circ} \qquad \text{(Eq. 4)}$$

ρ° :density of solvent
$\bar{\nu}$:partial specific volume of solute (cm^3/g)

Fig. 20. (a) Concentration dependence of the solution volume.
(b) Dependence of the solution density, ρ, on molarity of solute, c_2.

Partial molar volume of proteins and peptides

It is empirically known that the partial molar volume of various proteins can be calculated, as first proposed by Cohn and Edsall (1943) [56-58], for both native and denatured states using values of the partial molar volumes of each constituent amino

$$V_{\phi} = M\bar{\nu} = \sum_i N_i V_{\phi,i} \qquad \text{(Eq. 5)}$$

V_{ϕ} :Partial molar volume /cm^3mol^{-1}
M :Molecular weight of a protein
$\bar{\nu}$:Partial specific volume /cm^3g^{-1}
N_i :Partial molar volume of i th amino acid
$V_{\phi,i}$:number of i amino acid

Fig. 21(a). Calculation of V_{ϕ} for proteins proposed by Cohn et al[56].

Talbe II Partial molar volume of amino acid residues (Cohn&Edsall, 1943)

amino acid	$V_{\phi,i}$ /cm^3mol^{-1}
Gly	43.5
Ala	60.6
Val	92.7
Leu	108.4
Phe	121.3
Ser	60.8
Met	105.1
Trp	144.1
Asp	74.1
Asn	78.0
Gln	93.9
Lys	108.5
His	99.3
Pro	81.0

acid residue (Fig. 21 and Table II). This has been practice to assume the additivity of partial molar volumes of amino acid residues and to summing up the partial molar volumes of constituent amino acid residues. Another estimation of the partial molar volume of proteins was proposed using the values of constituent such as side-chains and the peptide groups (Eq. 6) [57, 58]. Likewise, the calculation of the partial molar volume including the contribution of the amino and carboxyl terminal groups to the partial molar volume were also available(Eq. 7). The calculated partial molar volume of $(Pro\text{-}Pro\text{-}Gly)_n$ and $(Pro\text{-}Hyp\text{-}Gly)_n$ (n=5,10) at 25 °C was indicated in Table III. In

$$V_\phi(cal) = (N-1)\,V_\phi(\text{-}CHCONH\text{-}) + \sum_{i=1}^{N} V_\phi(\text{-}R_i\text{-}) \quad \text{(Eq. 6)}$$

$$V_\phi(cal) = (N-1)\,V_\phi(\text{-}CHCONH\text{-}) + \sum_{i=1}^{N} V_\phi(\text{-}R_i\text{-}) + V_\phi(\text{-}CHCOOH) + V_\phi(\text{-}NH_3) \quad \text{(Eq. 7)}$$

$V_\phi(cal)$:calculated partial molar volume /cm^3mol^{-1}
N :the number of amino acid residues
$V_\phi(\text{-}CHCONH\text{-})$:contribution of a peptide unit /cm^3mol^{-1}
$V_\phi(\text{-}R_i\text{-})$:contribution of the i th amino acid side chain /cm^3mol^{-1}
$V_\phi(\text{-}NH_3)$:contribution of a amino terminal /cm^3mol^{-1}
$V_\phi(\text{-}CHCOOOH)$:contribution of a carboxyl terminal /cm^3mol^{-1}

Fig. 21(b). Calculation of V_ϕ for proteins using amide and amino acid side cahins (Eq. 6) and using amide, amino acid side cahins and both terminals.(Eq. 7).

this calculation, the contribution of terminal groups was estimated by subtracting the calculated partial molar volume according to Eq. 6.from the observed partial molar

Table III Calculated partial molar volumes* of collagen model peptides at 25 °C

Peptide	Cohn & Edsall(1943)[56]	Zamyatnin(1984)[57]	Makhatadze & Privalov(1943)[56,#]
$(ProProGly)_5$	900 (0.722)	921 (0.706)	830 (0.651)
$(ProProGly)_{10}$	1800 (0.727)	1841 (0.711)	1660 (0.656)
$(ProHypGly)_5$	932 (0.693)		834 (0.616)
$(ProHypGly)_{10}$	1865 (0.688)		1667 (0.620)

* expressed in cm^3mol^{-1} and the values in the parentheses is the partial specific volume /cm^3g^{-1}.

calculated by eq. 7 and the contribution of amide and side chains of Glycine and Proline was 28, 10.3 and 35.8 cm^3mol^{-1}. Total contribution of amino and carboxyl terminal was estimated from $V_{\phi,cal}$(Gly-Gly-Gly)-$V_{\phi,obs}$(GlyGlyGly) and was 28.6cm^3mol^{-1}.

volume of GlyGlyGly.

The conformation changes such as unfolding of proteins is thought to have little effect on the partial molar volumes and these calculations have been commonly used [58-60]. Density measurements normally require a large amount of sample and due to difficulty in determining the precise concentration of protein or peptide solutions, information on the partial molar volumes has not yet been readily available. Especially at high temperature, the limitation of instrumentation and the low solubility of most proteins in the denatured state prevent us from performing precise density measurement.

As shown in table III, large discrepancies between three methods and, even if one of the values is almost the correct value, it must be valid only for unfolded state (single chain). The partial molar volumes of collagen model peptides in the three stranded triple helix may be different from the value in the single chain and is indespensable in several physico-chemical studies such as ultracentrifugation or calorimetry.

In the present study, therefore, the author measured the density of solutions of $(Pro\text{-}Pro\text{-}Gly)_n$ and $(Pro\text{-}Hyp\text{-}Gly)_n$ (n=5, 10) in the temperature range from 5 °C to 85 °C. In case of these collagen model peptides, both tree stranded triple helix and single chain are highly soluble in the aqueous system, especially in the aqueous acetic acid solution, in this temperature range. Based on the precise concentration and density determinations, the partial molar volumes of both three stranded triple helix and single chains were obtained within this temperature range.

IV-2 Experimental

Sample preparations

$(Pro\text{-}Pro\text{-}Gly)_n$ and $(Pro\text{-}Hyp\text{-}Gly)_n$ (n=5, 10) were purchased from Peptide Inc (Mino Osaka, Japan). Samples were dissolved in pure water and dialyzed in the dialysis tube with a molecular cut off of 500 against pure water to remove salts and other small compounds. The purity of the peptides was higher than 99% for $(Pro\text{-}Pro\text{-}Gly)_n$ (n=5 ,10) and $(Pro\text{-}Hyp\text{-}Gly)_5$ and 98% for $(Pro\text{-}Hyp\text{-}Gly)_{10}$ as determined from the reverse phase HPLC (Shimadzu, LC10A). For all measurements, freeze-dried peptides were weighed, dissolved in 0.1M acetic acid, and the solutions were heated up to 80 degrees and kept there for 10 min. and then cooled to the room temperature for annealing. The solutions were kept at 4 degree at least 2weeks and degassed at 4 degree before the measurements were taken.

Concentrations of the protein and peptide solutions

In general, physico-chemical measurements of solutions require an accurate determination of the concentration in solution. This is especially important in the case of the determination of the partial specific volume. The partial specific volume for most proteins is about $7\times10^{-1}cm^3g^{-1}$, where the deviation arising from an error of 10% in the concentration of the solution becomes $7\times10^{-2}cm^3g^{-1}$ of the value. The partial specific volume changes induced by conformational transition of common proteins are usually less than 5×10^{-2} cm^3g^{-1}. This error in concentration causes serious problems when using partial specific volume determinations in studying conformational change. Proteins or peptides, whether in powder or crystal state, are not free of solvent molecules or salts. In this study, the author has performed precise amino acid analyses for all peptides studied, and the water contents were evaluated for each of the powder samples prepared. More than 15 solutions were analyzed for each peptide solution and the weight fraction of water is determined for the freeze-dried samples (powder). The average value of the glycine concentration obtained from amino acid analysis was employed to calculate the water content of the samples.

Density measurements

The precise densities of the solutions were determined by using vibrational densitymeter, DMA 5000 (Anton PAAR) using the tuning fork method (Fig. 22). This method yields a sufficiently high degree of accuracy (5×10^{-6}) and requires a comparatively small amount of solution (about $0.8cm^3$). The solution is placed in a U-shaped tube that can oscillate at a natural frequency. From this frequency, the density of the solution in the tube can be obtained using Eq.8. In this instrument the U-shaped tube is kept at a constant temperature (within ±0.01 °C) in the temperature range from 0 to

90. The frequency of the tube is given to 7 significant figures and hence the density of the solution can be found to 6 significant figures. Consequently, the concentration of the collagen model peptides can be obtained within an accuracy of 4 significant digits, and the partial molar volume can be estimated with 3 digits.

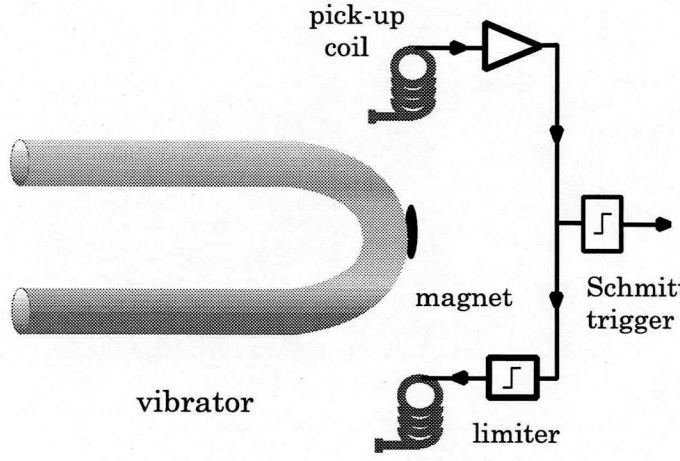

$$2\pi f=\sqrt{\frac{k}{m}}=\sqrt{\frac{k}{M_0+\rho V}} \qquad \text{(Eq. 8)}$$

f :resonant frequency
m :total mass
k :constant of elasticity of the spring
ρ :density of the sample
M_0 :effective mass of the empty vibrator
V :volume of the sample

Fig.22. Excitation system of the vibrational density meter

IV-3 Results and discussion

Water content of collagen model peptides

The water contents of collagen model peptides obtained from amino acid analyses were shown in Fig.23 and Table IV. From these values, the author could calculate the concentration of $(Pro\text{-}Pro\text{-}Gly)_n$ and $(Pro\text{-}Hyp\text{-}Gly)_n$ (n=5,10). The water content of $(Pro\text{-}Pro\text{-}Gly)_{10}$ obtained from precise amino acid analyses was 17.5 % and this value is

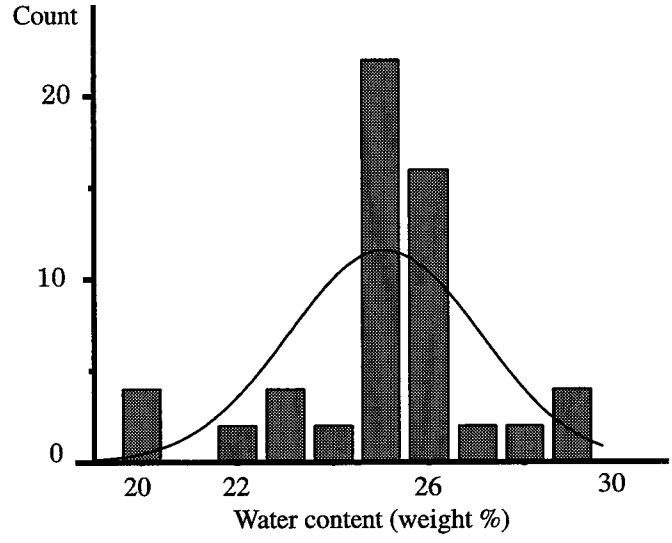

Fig.23. Histogram of water content of $(Pro\text{-}Hyp\text{-}Gly)_{10}$ determined from amino acid analysis.

Table IV Water contents (weight %) determined from amino acid analysis

Peptide	contents
$(Pro\text{-}Pro\text{-}Gly)_5$	21.6 ± 1.8
$(Pro\text{-}Pro\text{-}Gly)_{10}$	17.5 ± 1.8
$(Pro\text{-}Hyp\text{-}Gly)_5$	22.5 ± 1.2
$(Pro\text{-}Hyp\text{-}Gly)_{10}$	26.1 ± 1.9

in good agreement with the value reported by Engel et al. On the other hand, the water content of $(Pro\text{-}Hyp\text{-}Gly)_{10}$ obtained here is much higher than that obtained by Engel et al [16].

Partial specific volume of collagen model peptides

As shown in Fig. 24, linear relationships between the concentration and density for all the polypeptide solutions were obtained for the temperature and the concentration range studied. The partial molar volume of collagen model peptides at each temperature can be obtained from these relationships. In this chapter, the partial molar

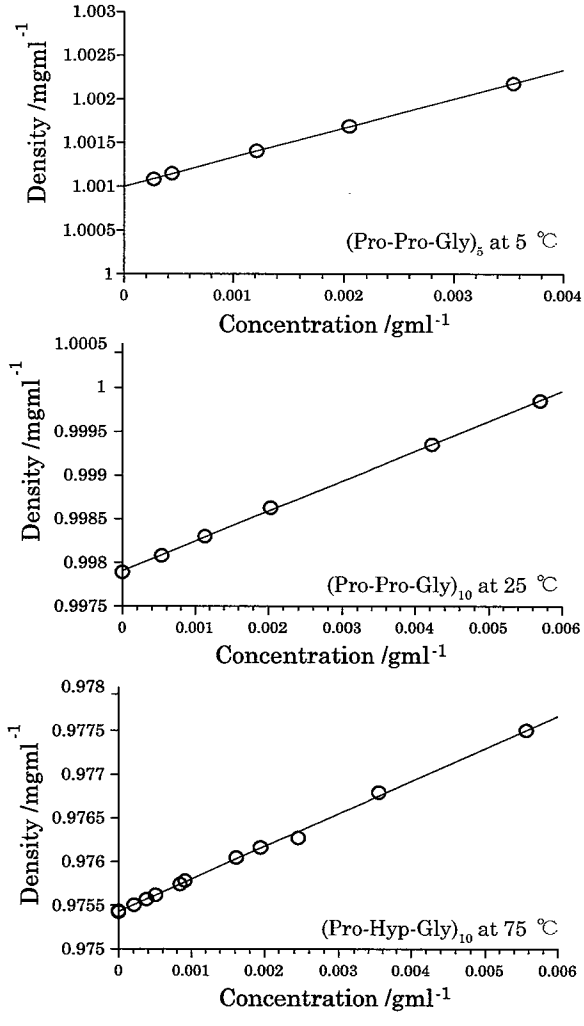

Fig. 24. Concentration dependence of the density for collagen model peptide solutions

volumes of the collagen model peptides were expressed per mole tripepide unit.

The partial molar volume of $(Pro\text{-}Pro\text{-}Gly)_5$ and $(Pro\text{-}Hyp\text{-}Gly)_5$ obtained here were listed in table V and plotted against the temperature in Fig. 25. The partial molar volume of both peptides increased as the temperature increasing. The partial molar volume of $(Pro\text{-}Hyp\text{-}Gly)_5$ had a large value of about 3.3 cm^3mol^{-1}, when compared to the value of $(Pro\text{-}Pro\text{-}Gly)_5$.

The contribution of hydroxyl group (-OH) could be estimated from the difference of two groups and is shown in Table VI [56-58,61,62]. Thus the difference in the partial molar volume between $(Pro\text{-}Pro\text{-}Gly)_5$ and $(Pro\text{-}Hyp\text{-}Gly)_5$ can be thought of as the contribution of hydroxyl group of the Hyp residue.

Table V Partial molar volume, V_ϕ of $(ProProGly)_5$ and $(ProHypGly)_5$

peptide	5℃	15℃	25℃	35℃	45℃
$(ProProGly)_5$	164.0(0.6436)	167.0(0.6551)	168.6(0.6614)	170.7(0.6696)	171.5(0.6730)
$(ProHypGly)_5$	166.3(0.6137)	169.9(0.6272)	171.9(0.6347)	175.0(0.6461)	174.2(0.6432)

55℃	65℃	85℃
172.3(0.6760)	174.8(0.6859)	
175.2(0.6469)	178.2(0.6580)	175.9(0.6495)

These values is in cm^3 per moltripeptide.The value in the parenthesis is the partial specific volume in cm^3g^{-1}.

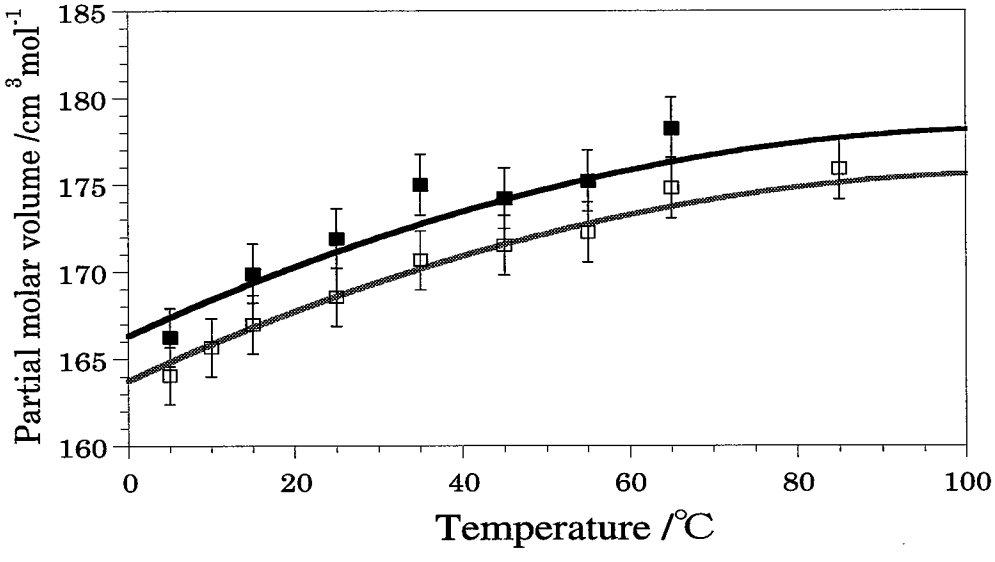

Fig. 25. Temperature dependence of the partial molat volume of (Pro-Pro-Gly)$_5$ (□) and (Pro-Hyp-Gly)$_5$ (■). The solid lines are obtained by polynominal least squares fits of the experimental values and the partial molarvolume functions, V_ϕ are;

$V_{\phi,(Pro\text{-}Pro\text{-}Gly)5}(T)=163.8+0.2187T-0.001T^2$

$V_{\phi,(Pro\text{-}Hyp\text{-}Gly)5}(T)=166.3+0.2187T-0.001T^2$

In contrast to the temperature dependence of the partial molar volume of (Pro-Pro-Gly)$_5$, the partial molar volume of (Pro-Pro-Gly)$_{10}$ increased sigmoidaly and showed cooperative transition with increasing temperature as shown in Fig. 26. The values at each temperature were indicated in table VII. The temperature range and transition temperature of this cooperative transition corresponded to the temperature

Table VI Contribution of -OH group to the partial molar volumes at 298.15 K.

Method	V_ϕ(-OH)-V_ϕ(-H) /cm^3mol^{-1}	References
V_ϕ(poly(Hyp))-V_ϕ(poly(Pro))	2.3	61
V_ϕ(Ser)-V_ϕ(Ala)	0.7	58
V_ϕ(Ser)-V_ϕ(Ala)	2.3	57
V_ϕ(-CH_2OH)-V_ϕ(-CH_3)	1.7	62
V_ϕ(-CHOH-)-V_ϕ(-CH_2-)	0.5	62
Average	1.5(0.9)	
V_ϕ(-Pro-Hyp-Gly-)-V_ϕ(-Pro-Pro-Gly-)	3.3	*

* The present work.

obtained from other experiments, such as sedimentation equilibrium or circular dichroism measurements. Consequently, this transition can be regarded as the transition from the three stranded triple helix to single chains of this collagen model peptide [7,16]. The difference in the partial molar volume between the three stranded triple helix and single chains of $(Pro\text{-}Pro\text{-}Gly)_{10}$ was 5.8 cm^3 mol^{-1} as indicated in Fig. 26.

Similar to the results of $(Pro\text{-}Pro\text{-}Gly)_{10}$, the partial molar volume of $(Pro\text{-}Hyp\text{-}Gly)_{10}$ also indicated the cooperative transition from the three stranded triple helix to single chains. The difference in the partial molar volume of $(Pro\text{-}Hyp\text{-}Gly)_{10}$ was 11.6 cm^3mol^{-1} and this value was about 2 times that of the $(Pro\text{-}Pro\text{-}Gly)_{10}$.

The partial molar volumes of constituent groups at each temperature were also reported by Privalov et al [58]. From these values, the partial molar volume of $(Pro\text{-}Pro\text{-}Gly)_n$ (n=5,10) at different temperature were calculated according to Eq. 7 and are plotted in Fig. 27 against temperature. At around room temperature, the

TableVII Partial molar volume, V_ϕ of $(ProProGly)_{10}$ and $(ProHypGly)_{10}$

peptide	10℃	15℃	25℃	35℃	45℃
$(ProProGly)_{10}$	169.4(0.6692)	169.7(0.6704)	170.4(0.6732)	172.4(0.6812)	174.5(0.6896)
$(ProHypGly)_{10}$	164.7(0.6120)	165.3(0.6141)	165.7(0.6158)	165.7(0.6158)	165.4(0.6146)

55℃	60℃	65℃	70℃	75℃	85℃
176.0(0.6955)	175.9(0.6952)		177.4(0.7008)		
168.6(0.6264)	174.8(0.6497)	169.5(0.6301)	175.1(0.6509)	178.1(0.6618)	178.23(0.6624)

These values is in cm^3 per moltripeptide.The value in the parenthesis is the partial specific volume in cm^3g^{-1}.

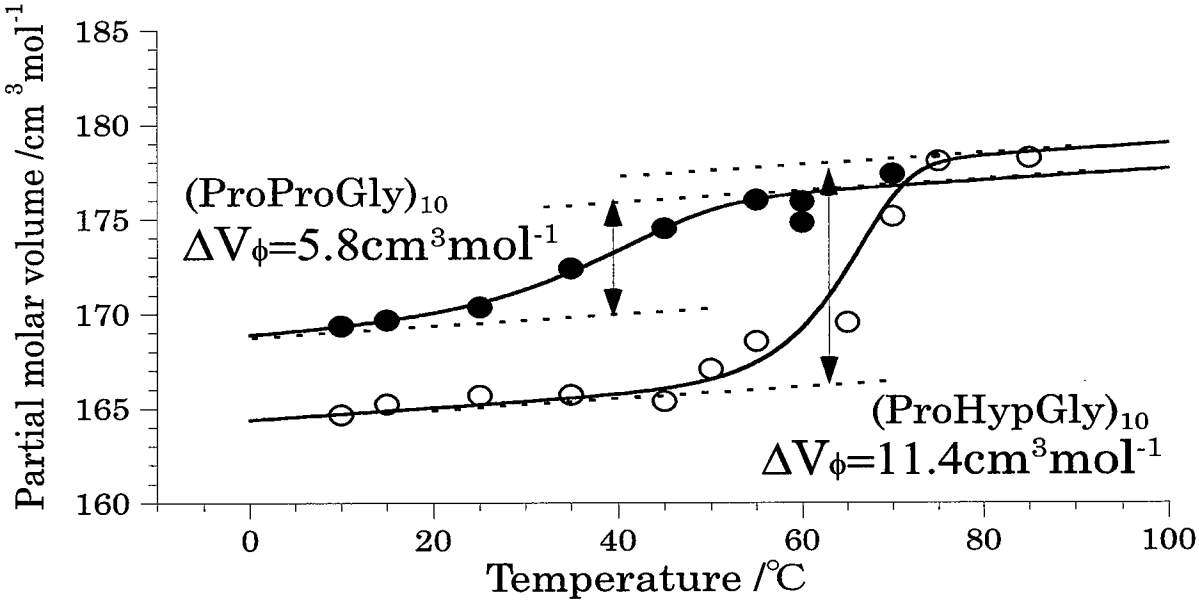

Fig. 26. Temperature dependence of the partial molar volume of (Pro-Pro-Gly)$_{10}$ and (Pro -Hyp-Gly)$_{10}$ The solid lines are results of a nonlinear least-squares fittng. The fittting was done by assuming two state transition (van't Hoff) and performing succesive iterations using Marquardt-Levenberg routine as available Mathematica 3.0.

observed partial molar volumes of collagen model peptides are not so different from the calculated values. On the other hand, regarding the temperature dependences of these peptides, large discrepancies are observed between observed and calculated values. Mostly, in case of the partial molar volume of (Pro-Pro-Gly)$_{10}$, cooperative

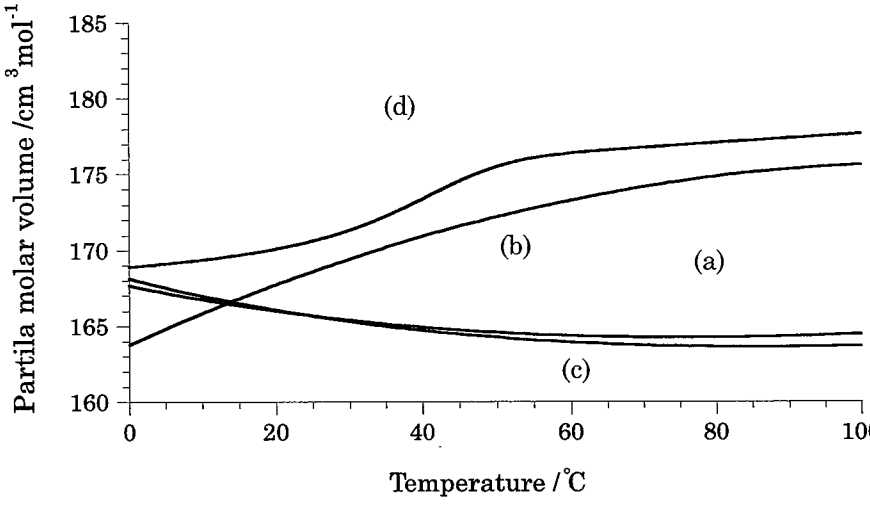

Fig. 27. Temperature dependence of the partial specific volume of (ProProGly)$_5$ and (ProProGly)$_{10}$. Calculated value (a) and observed value (b) of (ProProGly)$_5$ and calculated value (c) and observed value (d) of (ProProGly)$_{10}$.

volume increase are found which is caused by the transition from three stranded triple helix to single chains.

In contrast to the case of the transition from the native to denatured state of common proteins, large changes in the partial molar volume were observed for the transition of collagen model peptides from the three stranded triple helix to single chains. The three chains of collagen model peptides intertwine to forms rod-like triple helix structure, where the glycine residues are placed within the central portions of the triple helix (Fig 5). In contrast, the proline residues are positioned on the peripheral surface of the triple helix, facing outwards toward the solvent in a compact fashion. As the triple helix unwinds to single chain, the glycine residues are exposed to the solvent and this change in conformation induces the increase of the partial molar volume of collagen model peptides.

Conclusion

Several new and important discoveries about the transition of the triple helix to single chains of collagen model peptides have been obtained using various physico-chemical methods. The author has found in differential scanning calorimetry studies, especially from the specific heat capacity curves and the raising rate dependence of the transition, that the thermal transition of collagen model peptides exhibit an phase transition. Furthermore, the author succeeded in evaluating thermodynamic quantities of the transition from the triple helix to single chains, based on detailed studies of the raising rate dependence of the heat capacity curves. The transition temperature of $(Pro\text{-}Hyp\text{-}Gly)_{10}$ is found to be higher than that of $(Pro\text{-}Pro\text{-}Gly)_{10}$ and $(Pro\text{-}Hyp\text{-}Gly)_{10}$ is more stabilized because of a larger enthalpy difference between two states.

From the determination of the temperature dependence of the partial molar volumes of collagen model peptides it was found that the partial molar volumes increase markedly as the transition proceeds. The increase in the partial molar volumes of $(Pro\text{-}Hyp\text{-}Gly)_{10}$ was found to be distinctly larger than that of $(Pro\text{-}Pro\text{-}Gly)_{10}$. This is another important physical quantity, which directly indicates the difference in the nature of the transition of $(Pro\text{-}Pro\text{-}Gly)_{10}$ and $(Pro\text{-}Hyp\text{-}Gly)_{10}$. At the same time this difference is closely related to the difference in the ratio of the entropy change of the transition to the enthalpy change of the transition which in turn determines the transition temperature.

Another finding made by the author using NMR, the low temperature triple helix – high temperature triple helix transition, is still under investigation. Briefly, the author has found that this transition accompanies absorption of heat at a specific temperature irrespective of the solution system studied.

References

[1] Linsenmayer, T. F. (1991) *Cell Biology of Extracellar Matrix 2nd ed.*, Hay, E. D., Ed., New York : Plenum Press, pp.7-44

[2] Rich, A. and Crick, F.H.C. (1955) *Nature* 176, 915.

[3] Ramachandran, G.N. and Kartha, G. (1955) *Nature* 176, 593.

[4] Brodsky-Doyle, B., Leonard, K.R. and Reid, K.B., (1976) *Biochem. J.* 159, 279.

[5] Kodama, T., Freeman, M., Rohrer, L., Zabrecky, J., Matsudaira, P. and Krieger, M.(1990) *Nature* 343, 531.

[6] Rich, A. and Crick, F.H.C. (1961) *J .Mol. Biol.* 3, 483.

[7] Kobayashi, Y., Sakai, R., Kakiuchi, K. and Isemura, T. (1970) Biopolymers 9, 415.

[8] Sakakibara, S., Inoue, K., Shudo, K., Kishida, Y. Kobayashi., Y. and Prockop, D.J. (1973) *Biochim. Biophys. Acta* 303, 198-202.

[9] Fields, G.B. and Prockop, D.J. (1996) *Biopolymers* 40, 345.

[10] Okuyama, K., Okuyama, K., Arnott, S., Takayanagi, M., and Kakudo, M. (1981) *J. Mol. Biol* 152, 427-443.

[11] Bella, J., Eaton, M., Brodsky, B. and Berman, H.M. (1994) *Science* 266, 75

[12] Bella, J., Brodsky, B. and Berman, H.M. (1995) *Structure* 3, 893

[13] Kramer, R. Z., Vitagliano, L., Bella, J., Berisio, R., Mazzarella, L., Brodsky, B.,Zagari, A., and Berman, H. M. (1998) *J. Mol. Biol.* 280, 623-638.

[14] Nagarajan, V., Kamitori, S., and Okuyama, K. (1998) *J. Biochem.* 124, 1117-1123.

[15] Lazarev, Y. A., Grishkovsky, B.A., Khromova, T. B., Lazareva, A. and Grechishko, V. S. (1992) *Biopolymers* 32, 189.

[16] Engel, J., Chen, H.T., Prockop, D.J. and Klump, H. (1977) *Biopolymers* 16, 601.

[17] Li, M.H., Fan, P., Brodsky, B. and Baum, J. (1993) *Biochemistry* 32, 7377-7387.

[18] Long, C.G., Braswell, E., Zhu, D., Apigo, J., Baum, J. and Brodsky, B. (1993) *Biochemistry* 32, 11688.

[19] Feng, Y., Melacini, G., Taulane, J. P. and Goodman, M. (1996) *Biopolymers* 39, 859.

[20] Feng, Y., Melacini, G. and Goodman, M. (1997) *Biochemistry* 36, 8716.

[21] Nemethy, G. and Scheraga, H.A. (1984) *Biopolymers* 23, 2781-2799

[22] Burjanadze, T. V. (1992) *Biopolymers* 32, 941-949

[23] Nemethy, G., Gibson, K. D., Palmer, K. A., Yoon, C. N., Paterlini, G., Zagari, A., Rumsey, S. and Scheraga, H. A. (1992) *J. Phys. Chem.* 96, 6472

[24] Brandts, J.F. and Lin, L. (1990) *Biochemistry* 29,6927.

[25] Scholtz, J.M, Marqusee, S., Baldwin, R.L., York, E.J, Stewart, J.M., Santoro, M.M. and Bolen, D.W. (1991) *Proc. Natl. Acad. Sci. U.S.A.* 88, 2854.

[26] Privalov, P.L. and Potekhin, S.A. (1986) *Methods in Enzymology* 131, 4.
[27] Gibbs, J.H. and DiMarzio, E. A. (1959) *J. Chem. Phys.* 30, 271.
[28] Zimm, B. H. and Bragg, J. K. (1959) *J Chem. Phys.* 31, 526.
[29] Lifson, S. and Roig, A. (1961) *J Chem. Phys.* 34, 1963.
[30] Poland, D. and Scheraga, H. (1966) *J Chem. Phys.* 45, 1456.
[31] Poland, D. and Scheraga, H. (1966) *J Chem. Phys.* 45, 1464.
[32] Grosberg, A.Y. and Khokhov, A. R. (1994) *Statistical physics of macromol ecules*, AIP, New York.
[33] Sutoh, K. and Noda, H. (1975) *Biopolymers* 13, 2477.
[34] Shaw, B. R. and Schurr, M. (1975) *Biopolymers* 14, 1951.
[35] Freire, E., van Osdel, W. W., Mayorga, O. L. and Sanchez-Ruiz, J. M. (1990) *Ann. Rev. Biophys. Biophys.* 19, 159.
[36] Privalov, P.L. (1980) *Pure Appl. Chem.* 52, 479.
[37] Sturtvant, J. M. (1987) *Ann. Rev. Phys. Chem.* 38, 463.
[38] Scholtz, J. M, Marqusee, S. Baldwin, R. L. York, E. J. Stewart, J. M., Santoro, M.M. and Bolen., D. W. (1991) *Proc. Natl. Acad. Sci. U. S. A.* 88, 2854.
[39] Privalov, P.L. (1979) *Adv. Protein Chem.* 33,167.
[40] Makhatadze, G.I. and Privlov, P.L. (1990) *J. Mol. Biol.* 213, 375.
[41] Makhatadze, G.I. Medvedkin, V.N. and Privlov, P.L. (1990) *Biopolymers* 30, 1001
[42] Lumry, R. and Rajender, S. (1970) *Biopymers* 9, 1125.
[43] Slijper, M. Bonvin, A. M. Boelens, R. and Kaptein, R. (1996) *J. Mol. Biol.* 259, 761.
[44] Arcus, V. L. Vuilleumier, S. Freund, S. M. Bycroft, M. and Fersht, A. R. (1995) *J. Mol. Biol.* 254, 305.
[45] Kobayashi, Y. and Kyogoku, Y. (1973) *Biopolymers* 81, 337-347.
[46] Brodsky, B., Li, M.H., long, C.G. Apigo, J. and Baum, J. (1992) *Biopoly mers* 32, 447.
[47] Rance, M., Sorensen, O.W., Bodenhausen, G., Wagner, G., Ernst, R.R. and Wuthrich, K. (1984) *Biochem.Biophys.Res.Commun.* 117, 479-485
[48] Hurd, R. E. and John, B. K. (1991) *J. Magn. Reson.* 91, 648.
[49] Bothner, A. A., Stephens, R. L., Lee, J., Warren, C. D. and Jeanloz, R.W., (1984) *J. Am. Chem. Soc.* 106, 811.
[50] Kobayashi, Y., Kyogoku, Y. and Inoue, K. (1982) *Abstract, 10th Int. Conf. on Magnetic Resonance in Biological Systems*, Stanford, CA, p. 179.
[51] Kemp, D. S. (1979) *The Peptides: Analysis, Synthesis, Biology, vol. 1,* Academic Press, New York, , p315.

[52] Poznanski, J., Ejchart, A., Wierzchowski, K.L. and Ciurak, M. (1993) *Biopolymers* 33, 781-795.

[53] Raligh, D.P., Evans, P.A. Pitkeathly, M. and Dobson, C. M. (1992) *J. Mol. Biol.* 228, 338.

[54] Patel, D.J. Pardi, A. and Itakura, K. (1982) *Science* 216, 581.

[55] Eisenberg, H. (1976) In *Biological Macromolecules and Polyelectrolytes in solu tion*, Oxford : Clarendon Press.

[56] Cohn, E. J., Edsall, J. T. (1943) In *Proteins, Amino Acids and Peptides*, New York : Reinhold, 155-176.

[57] Zamyatnin, A. A. (1984) *Annu. Rev. Biophys. Bioeng.* 13, 145-165.

[58] Makhatadze, G. I., Medvedkin, V. N., and Privalov, P. L. (1990) *Biopolymers* 30, 1001-1010.

[59] Chalikian, T. V., Volker, J., Anafi, D., and Breslauer, K. J. (1997) *J. Mol. Biol.* 274, 237-252.

[60] Chalikian, T. V., Totrov, M., Abagyan, R., and Breslauer, K. J. (1996) *J. Mol. Biol.* 260, 588-603.

[61] Knof, S., and Engel, J. (1974) *Israel J. Chem.* 12, 165-177.

[62] Durchschlag, H. (1986) *Thermodynamic Data for Biochemistry and Biotechnology*, Hinz, H.-J., Ed., Berlin: Springer-Verlag, pp 45-128.

List of publications

Uchiyama, S., Kai, T., Kajiyama, K., Kobayashi, Y., and Tomiyama, T. (1997). Mea surement of thermodynamic quantities in the heating-rate dependent thermal transitions of sequenced polytripeptides. *Chem. Phys. Lett.* 281, 92-96.

Kai, T., Uchiyama, S., Kajiyama, K., Kobayashi, Y., and Tomiyama, T. (1997). NMR observation of two states of triple helix in the thermal transition of (Pro-Pro-Gly)10. *Chem. Phys. Lett.* 281, 86-91.

Kajiyama, K., Tomiyama, T., Uchiyama, S., and Kobayashi, Y. (1995). Phase tranasitions of sequenced polytripeptides observed by microcalorimetry. *Chem. Phys. Lett.* 247, 299-303.

Related publications

Ogawa, K., Nishimura, S., Uchiyama, S., Kobayashi, K., Kyogoku, Y., Hayashi M., and Kobayashi, Y. (1998). Conformation analysis of eel calcitonin. *Eur. J. Biochem.* 257, 331-336.

Tomiyama, T., Uchiyama, S., and Shinohara, H. (1997). Solubility and partial specific volume of C_{60} and C_{70}. *Chem. Phys. Lett.* 264, 143-148.

Acknowledgements

The studies presented in this thesis have been performed under the direction of Professor Yuji Kobayashi, Graduate School of Pharmaceutical Sciences, Osaka University and Dr. Tetsuo Tomiyama, Graduate School of Science, Nagoya University.

The author is indebted to my teachers, colleagues and co-workers, who have provided his inspiration, criticism and enlightenment for my work. The author would like to express my sincere gratitude to Professor Yuji Kobayashi and Dr. Tetsuo Tomiyama for their cordial guidance and helpful criticism and encouragement. In the preparation of this thesis the author has greatly benefited from the advice of Dr. Tetsuo Tomiyama.

The present research owes much to the precise amino acid analysis performed by Dr. Yoshiko Yagi (Institute for protein science, Osaka University).

The author also wishes to thank Mr. Koichi Kajiyama (President of Admon Science Inc. Fujieda) for providing me with instruments and valuable advice. The author wishes to express my gratitude to Professor Hisanori Shinohara (Graduate School of Science, Nagoya University) for helpful comments. Thanks are also due to Dr. Eugene Permyakov (Russian Academy of Science) for his suggestion regarding instrumentation. Special thanks are due to Kazuhiro Fukada (Tokyo Metropolitan University) for allowing use of his density meter and expertise. The author also wishes to thank Professor Yoshimasa Kyogoku (Institute for Protein Research, Osaka University) and Dr. Tadayasu Ohkubo (Pharmaceutical Sciences, Osaka University) for helpful advices. Thanks are also due to Professor Takeshi Imanishi, Professor Motomasa Kobayashi and Professor Hidenobu Omori (Pharmaceutical Sciences, Osaka University) for reading the draft and making a number of helpful suggestions. The author gratefully acknowledge helpful discussions with Takuya Yoshida (Pharmaceutical Sciences, Osaka University), Tsutomu Kai and Yoshinori Nishi (Graduate School of Science, Nagoya University). Finally, thanks are also due to Hideto Shimahara, Tetsuya Ishino, Tomohisa Hatta, Kaoru Kobayashi and all members of the Laboratory of Physical Chemistry of Pharmaceutical Sciences.

Lastly, I thank my wife Izumi for her understanding and support during the course of this work. And I wish to thank my parents for their care and support.